Title

Plasticity and not adaptation is the primary source of temperature-mediated variation in flowering phenology in North America

Journal

Nature Ecology & Evolution, 8(3)

ISSN

2397-334X

Authors

Ramirez-Parada, Tadeo H
Park, Isaac W
Record, Sydne
et al.

Publication Date

2024-03-01

DOI

10.1038/s41559-023-02304-5

Peer reviewed

Title: Plasticity and not adaptation is the primary source of temperature-mediated variation in flowering phenology in North America

Authors: Tadeo H. Ramirez-Parada[1], Isaac W. Park[1], Sydne Record[2], Charles C. Davis[3], Aaron M. Ellison[3,4], Susan J. Mazer[1]

Institutional Affiliations: [1]Department of Ecology, Evolution, and Marine Biology, University of California, Santa Barbara, CA 93106, USA. [2]Department of Wildlife, Fisheries, and Conservation Biology, University of Maine, Orono, ME, 04469, USA. [3]Department of Organismic and Evolutionary Biology, Harvard University, Cambridge, MA 02138, USA. [4]Sound Solutions for Sustainable Science, Boston, MA 02135, USA.

Corresponding Author: Tadeo H. Ramirez-Parada, (+1) 504-638-5792, tadeoramirezp@gmail.com

Running title: Plasticity, not adaptation, drives phenology

Number of figures: 4

Number of tables: 1

Supporting Information: 31

ABSTRACT

Phenology varies widely over space and time because of its sensitivity to climate. However, whether phenological variation is primarily generated by rapid organismal responses (i.e., plasticity) or local adaptation remains unresolved. Here, we used 1,038,027 herbarium specimens representing 1,605 species from the continental United States to measure flowering time sensitivity to temperature over time (‘S_{time}’) and space (‘S_{space}’). By comparing these estimates, we inferred how adaptation and plasticity historically influenced phenology along temperature gradients and how their contributions vary among species with different phenology and native climates, and among ecoregions differing in species composition. S_{space} and S_{time} were positively correlated (r = 0.87), of similar magnitude, and more frequently consistent with plasticity than adaptation. Apparent plasticity and adaptation generated earlier flowering in spring, limited responsiveness in late summer, and delayed flowering in fall in response to temperature increases. Nonetheless, ecoregions differed in the relative contributions of adaptation and plasticity, from consistently greater importance of plasticity (e.g., Southeastern USA Plains) to their nearly equal importance throughout the season (e.g., Western Sierra Madre Piedmont). Our results support the hypothesis that plasticity is the primary driver of flowering time variation along temperature gradients, with local adaptation having a widespread but comparatively limited role.

MAIN TEXT

The timing of life-cycle events (‘phenology’) determines the environmental conditions that organisms encounter throughout development and often mediates their fitness[1]. Phenology usually is cued by seasonally and interannually variable climatic factors—such as temperature—that enable individuals to adjust growth and reproduction plastically in response to fluctuating environmental conditions[1,2]. Phenology also varies within species as a result of evolutionary adaptation to local environments, which may select for different mean phenological timings among or within populations in space and time[3–6]. Although both plasticity and adaptation alter phenology, their relative contributions rarely have been measured within the same system largely because doing so requires experiments or spatiotemporally extensive genetic sampling[7–9] (but see [6]). Accordingly, most studies have highlighted either plasticity or adaptation as mechanisms of phenological variation attributable to environmental change[7], but their relative importance across species and ecological contexts remains unresolved. Elucidating the degree to which species have phenologically responded to historical climatic variation through plasticity or adaptation could provide important context for predicting whether organismal responses may be sufficient—or evolutionary change necessary—to maintain development synchronized with suitable climatic conditions in a warming world[8].

Phillimore et al.[9] proposed that the relative and joint contributions of plasticity and local adaptation to spatial variation in phenology within a species can be estimated from the difference between the slopes of spatial and temporal phenology-climate relationships. This proposition rests on several observations. The effects of interannual climatic variation on phenology generally reflect plastic responses, especially among long-lived species less liable to experience microevolutionary changes from year to year[10]. Phenological variation over space also can be caused by phenotypic plasticity where, for example, growing-degree day (GDD) thresholds that trigger life-cycle events occur on different dates across sites[11]. However, among populations, local adaptation also can generate phenological variation along climatic gradients[12,13]. Therefore, assuming no confounding factors, and absent significant variation in phenological plasticity within and among populations, phenological variation along spatial climate gradients should reflect the joint effects of plasticity and adaptation[14].

Given these observations and assumptions, plasticity and adaptation can generate five empirical patterns of sensitivity to temporal climatic variation (hereafter 'S_{time}') and to spatial climatic variation (hereafter 'S_{space}') (Fig. 1). First, if a species does not show phenological plasticity but population-level phenological means are locally adapted across a climatic gradient, we should observe negligible sensitivity to temporal climatic variation (i.e., no plasticity; $S_{time} = 0$) and a biologically significant difference between the slopes of the temporal and spatial relationships ($S_{space} - S_{time} \neq 0$ attributable to adaptation along the gradient; Figs. 1a,b). Alternatively, a phenologically plastic species whose populations are not locally adapted along the gradient should show biologically significant sensitivity to interannual climatic variation (i.e., $S_{time} \neq 0$) and no differences between temporal and spatial slopes ($S_{space} - S_{time} = 0$; Figs. 1c,d), implying that variation along the gradient can be attributed to plastic responses (i.e., $S_{space} = S_{time}$). When both adaptation and plasticity drive phenological variation along the climate gradient (i.e., $S_{time} \neq 0$ and $S_{space} - S_{time} \neq 0$), the resulting empirical pattern should depend on the relative direction of plastic and adaptive responses. Specifically, when adaptation operates in the same direction as plasticity (i.e., "co-gradient adaptation"), we should observe a greater spatial than temporal sensitivity (e.g., $S_{time} < 0$ and $S_{space} - S_{time} < 0$ implies that $S_{space} < S_{time}$, so S_{space} is more negative; Figs. 1e, f). In turn, when adaptation operates in the opposite direction as plasticity (i.e., "counter-gradient adaptation"[15,16]), we should observe a lesser spatial sensitivity or one of opposite direction to the temporal relationship (e.g., $S_{time} < 0$ and $S_{space} - S_{time} > 0$ implies that $S_{space} > S_{time}$, so S_{space} is either less steep, or positive; Figs. 1g, h). Finally, if a species shows no plasticity or local adaptation along a climate gradient, we would expect biologically non-significant temporal and spatial sensitivities (Figs. 1i, j).

Phenological sensitivity to temperature often varies among species occurring in different regions or that initiate phenological events at different times throughout the growing season[17–24]. However, comparisons of phenological sensitivity to climate over space and time—which are necessary to evaluate the apparent contributions of plasticity and adaptation (Fig. 1)—across species differing in phenology and occupying different climates require spatiotemporally extensive datasets and therefore remain rare. Herbaria provide abundant and increasingly available data to conduct these analyses at unprecedented taxonomic, temporal, and spatial scales[21,25–30]. However, few studies have separately estimated sensitivity to spatial versus temporal climate variation using specimens (but see[28,31–36]), and none have leveraged their unique scope to determine the ecological contexts in which plasticity or adaptation might contribute more strongly to spatial variation in phenology.

Here, we analyzed a dataset of over a million flowering specimens from 1,605 species across the continental United States to compare phenological sensitivities to spatial and temporal variation in temperature (‘S_{space}’ and ‘S_{time}’, respectively). For each species, we assessed whether its empirical sensitivity patterns were consistent with the effects of plasticity, adaptation, or both along temperature gradients (Fig. 1). Additionally, we evaluated how apparent temperature-related plasticity and adaptation of flowering time varied among species with different native climates, phenological niches, and occurring within different regional floras. Together, our analyses identified ecological contexts in which plasticity or adaptation appear to have most strongly influenced spatial phenological variation, providing the most taxonomically and geographically extensive assessment of temperature-mediated variation in flowering time among North American angiosperms conducted to date.

RESULTS

Plasticity vs. adaptation as determinants of phenology

S_{space} and S_{time} of 93% and 79% of species, respectively, differed from 0 with at least 95% probability. S_{space} and S_{time} agreed in direction for 94% of species and estimates of both S_{time} and S_{space} were negative for 89% and 91% of species, indicating earlier flowering across increasingly warmer locations and in warmer-than-average years (Fig. 2a).

Both apparent plasticity and adaptation were associated with clinal variation in flowering time along temperature gradients, with plasticity playing a predominant role among species. S_{space} and S_{time} were highly positively correlated, and their magnitude tended to correspond 1-to-1 for many species (Fig. 2b). Therefore, flowering shifts in warmer-than-average years typically had similar direction and magnitude (in days/°C) as those observed across increasingly warmer locations, consistent with a scenario of plasticity as the cause of phenological variation along spatial temperature gradients (Figs. 1c,d; Table 1).

More species showed sensitivity patterns consistent with plasticity (79%) than with adaptation (45%) (see Fig. 1, and a detailed classification scheme in Table 1). Apparent plasticity explained approximately 52% of the variance in flowering-time clines along temperature gradients among species (Fig. 2b). Fourty-one percent of species showed sensitivity patterns consistent with plasticity as the sole driver of phenological variation across gradients. In contrast, only 7% of species showed sensitivity patterns consistent solely with adaptation (see Figs. 1a,b). Thirty-eight percent of the species showed both apparent local adaptation and evidence of plasticity. Among these, a greater proportion showed flowering advances (and co-gradient patterns; 27%) than flowering delays (and counter-gradient patterns; 10%) resulting from apparent adaptation along temperature gradients (Fig. 2b). Fourteen percent of species showed patterns that were consistent neither with temperature-related plasticity nor with adaptation. These patterns remained consistent when analyzing only long-lived species (whose responses to yearly temperature anomalies are certain to be plastic) (Extended Data Fig. 1).

Plasticity and adaptation across ecological contexts

Apparent plasticity (S_{time}) varied substantially among species with different phenological niches and across local climates ($R^2 = 0.55$; Fig. 3a,c). Species flowering during late winter and spring tended to show flowering advances in warmer-than-average years. Such advances decreased in magnitude throughout the season, typically reversing to flowering delays during late summer and fall (Fig. 3a,c). The timing of the transition from positive values was consistent throughout PC1 (Fig. 3a), but occurred much earlier in arid regions with high temperature seasonality along PC2 (Fig. 3c). Apparent adaptation ($S_{space} - S_{time}$) also varied with phenological niche and native climate ($R^2 = 0.47$, Figs. 3b,d). Apparent adaptation varied from negative to positive values throughout the growing season, indicating a transition from flowering advances to delays attributable to local adaptation. Such transitions occurred much earlier in cool, thermally seasonal regions (i.e., the low range of PC1) (Fig. 3b). Apparent adaptation also varied throughout the growing season along PC2, with transition from advances to delays under warmer conditions occurring earlier in regions with high precipitation (Fig. 3d).

These patterns were mirrored at the regional level: throughout the season, average apparent plasticity and adaptation among species transitioned from generating flowering advances to generating delays in response to higher temperatures in all sampled ecoregions (R^2 for S_{time} = 0.44; R^2 for $S_{space} - S_{time}$ = 0.35; Fig. 4). This transition invariably occurred during the summer months. The magnitude of apparent adaptation tended to be lower than that of apparent plasticity during most of spring and early summer for all ecoregions, but their difference tended to be less among species flowering during early spring and the magnitude of adaptation was often greater among species flowering during late summer and early fall (Figs. 4a–n). Nonetheless, we detected regional differences in the relative contributions of apparent adaptation and plasticity among species throughout the season. For example, apparent adaptation and plasticity had similar magnitudes within the Western Sierra Madre Piedmont (Fig. 4g). In contrast, mean apparent plasticity was consistently greater than adaptation among species in the Southeastern USA Plains (Fig. 4j). The difference in magnitude between apparent plasticity and adaptation was greatest among early- to mid-summer flowering species in the Western Cordilleras and Cold Deserts (Figs. 4b, c).

DISCUSSION

This study provides evidence that, for 1605 North American plant species, phenotypic plasticity historically has been the primary mechanism generating flowering-time variation along temperature gradients. Nonetheless, apparent adaptation and plasticity jointly generated phenological variation in a large proportion of species. Both apparent plasticity and adaptation consistently generated flowering advances in spring, lesser advances during summer, and flowering delays during early fall, and this pattern was consistent across climates and ecoregions. Whether phenological reaction norms to historical climatic conditions will remain adaptive under future climatic regimes is unclear[10]. Nonetheless, these results suggest that plasticity historically has enabled flowering phenology to respond quickly to a wide range of temperature conditions among North American angiosperms, with adaptation frequently playing an important but context-dependent role.

Plasticity causes clinal variation in flowering time—Extensive research has documented phenological plasticity to spatial climatic variation in plants[37–40] that can result in clinal phenological variation even among short-lived taxa[11,41]. Our study extends these results by showing that the predominance of plasticity over adaptation associated with temperature-related variation in phenology over space might be the norm among North American species.

The greater importance of plasticity found in this study does not contradict the well-established role of phenological adaptation in space and time[40], which can mediate rapid temporal shifts in phenology[5] or facilitate ecological invasions[6,42]. Indeed, 45% of species in our data showed evidence of adaptation-driven phenological variation along temperature gradients (Fig. 2b). It is also possible that we did not detect non-linear or patchy adaptation patterns, or that the contributions of apparent adaptation and plasticity may be different in regions underrepresented in our data (e.g., the Great Plains and prairies; Extended Data Fig. 2). Crucially, we only assessed the apparent contributions of plasticity and adaptation to observed variation in flowering time over temperature gradients, so our results do not rule out the possibility that adaptation is the primary driver of phenological variation along gradients of different climatic variables. Finally, determining the exact environmental conditions within microsites where herbarium specimens were collected is impossible because continental-scale climate products have relatively coarse spatial resolution and because specimen coordinates typically are inexact. Climatic variation at the microsite level could confound our estimates of S_{space} and our assessment of the prevalence of local adaptation if, for example, different populations along the gradient occupied distinct microsites that maintained temperatures more constant than apparent when looking at coarser pixel-level averages. However, to our knowledge, such microsite sorting across species ranges has only been reported at their trailing edges where climate is most limiting[43]. Nonetheless, these potential complexities underscore the ultimate need for molecular or quantitative genetic studies to corroborate the broad correlational patterns outlined in this study.

Still, the strong correlation between S_{space} and S_{time} has important implications for phenoclimatic research. For example, it suggests that temperature-related variation in flowering time among conspecific populations is a good proxy of responsiveness to interannual temperature variation. Therefore, space-for-time substitutions might be viable approaches for quantifying plastic flowering responsiveness to temperature in North American angiosperms, for most of which we lack long-term phenological records[26,44]. Specifically, the match between S_{space}

and S_{time} shows that substituting space for time might reveal the direction and approximate magnitude on flowering sensitivity to temperature over time within species, or relative differences in sensitivity among species. However, co-gradient adaptation frequently generated spatial sensitivities of greater magnitudes than those over time, demonstrating that S_{space} might overestimate S_{time} in many species.

Our results also indicate that plasticity may have generated phenological variation across a temperature range (i.e., a median range of 13.7 °C) exceeding the degree of warming forecasted for most regions in coming decades. However, such historical plastic flowering shifts over space will not necessarily be mirrored by temporal shifts within populations as warming trends continue. For example, historical temperature cues may become uncorrelated from the factors mediating the fitness consequences of phenology, rendering plastic reaction norms maladaptive[3,10]. Plastic phenological shifts associated with warming also may be constrained by physiology[45] or by other competing cueing mechanisms such as photoperiod or winter chilling that may be disrupted by phenological shifts associated with higher temperatures[46–48]. These complexities highlight the need for research on the fitness consequences of recent and ongoing phenological shifts[49,50], and on the interrelated mechanisms underpinning associations between multiple abiotic cues (e.g., chilling, forcing, photoperiod, resources) and seasonal development beyond model systems[48,51].

Plasticity and adaptation vary across ecological contexts—Sensitivities transitioned from flowering advances under warming in spring to reduced or no responsiveness during summer and even flowering delays in early fall (Figs. 3, 4). This pattern implies that temperature trends will likely drive changes to the structure of the flowering season during spring and fall under global change, but that other environmental factors might play predominant roles during summer.

These results support studies showing decreases in phenological sensitivity to temperature among species throughout the season in temperate biomes[18,21,52,53], and others showing flowering delays among autumn-flowering species or lengthening of the growing and flowering seasons under warming[23,54–56]. While we cannot unambiguously identify the causes of this pattern, studies have shown that warming typically advances phenology during spring due to accelerated developmental rates, while phenophases occurring during fall are cued directly by seasonal cooling[57–59]. This difference would explain why fall-flowering species showed phenological delays under warming (i.e., fall cooling occurs later in warmer-than-average years), or why the transition from advances to delays was more pronounced within cool regions with high temperature seasonality (i.e., those showing more pronounced cooling during fall; Fig. 3). Regardless of its causes, our study corroborates that transitions from spring flowering advances to fall delays because of climatic warming are consistent across thousands of species and diverse climate zones and biomes in the continental United States.

Likewise, apparent adaptation throughout the season typically transitioned from generating mean flowering advances to generating delays along temperature gradients. Our results are consistent with those reported by Delgado et al.[23], who found changes in the direction of apparent plasticity and adaptation throughout the growing season for multiple trophic levels (i.e., saprotrophs, primary producers, and primary and secondary consumers) in Eastern Europe. That changes in apparent plastic and adaptive responses to warming throughout the year might be robust across different phenophases, taxa, trophic levels, or climatic regimes across the temperate zone may reflect shared cueing mechanisms or selective pressures for different phenological events occurring during the same seasons[56], with factors other than temperature (e.g., resources or photoperiod) likely driving phenological variation for developmental events in summer. Additionally, the greater prevalence of co-gradient adaptation as opposed to counter-gradient adaptation suggests that adaptation typically operates to generate greater variation in phenology along temperature gradients than generated by plasticity alone.

CONCLUSIONS

Our findings indicate that phenotypic plasticity is the predominant historical mechanism of spatial phenological variation across a wide range of temperature conditions in the continental United States; adaptation plays more context-specific roles. Whether and how species-level attributes such as functional traits and life history may mediate these relative contributions or whether historical responses will tend to be adaptive under non-analog climatic conditions remain open questions and important directions for future research. Our results outline broad correlational patterns whose verification will require direct measurements of plasticity and adaptation across species and climate regions. Nonetheless, our data—across many biomes and thousands of species—confirmed patterns of plastic and adaptive phenological advances in spring and delays in fall in response to warming observed in detailed empirical studies, highlighting the increasing utility of biological collections for studying plant responses to global change at vast taxonomic and spatiotemporal scales.

METHODS

Specimen data

We assembled specimen records from 220 herbaria made available digitally through 16 consortia from Mexico, the United States, and Canada (accessed during July and August of 2022; Note S1). We retained only specimens explicitly recorded as bearing flowers, which we determined by summarizing all unique entries in the DarwinCore 'reproductiveCondition' column and identifying those that unambiguously indicated presence of flowers. After harmonizing species names using the Taxonomic Name Resolution Service[60], we removed specimens lacking species-level identification, GPS coordinates, or dates of collection. To match the spatial and temporal coverage of the climate data (see ***Climate data*** below), we retained only specimens collected from 1896 to 2020 within the United States. We considered as duplicates any conspecific specimens collected within 111m (i.e., 0.001 of a decimal degree) of one another on the same date. For subsequent analysis, we selected species represented by at least 300 specimens to ensure that our model was computationally tractable and that we had sufficient sample sizes for estimating temperature responses in space and time. This filtering yielded a sample of 1,038,047 specimens from 1,605 species (Extended Data Fig. 2) (see [61] for additional methodological detail).

We used day of year ('DOY') of collection of each specimen as a proxy for flowering date. Because flowering spanned year-ends for many species, we accounted for the DOY discontinuity between December 31st and January 1st using an azimuthal correction, whereby DOYs from the year prior become negative values[29].

Climatic data

Temperature conditions preceding and leading up to anthesis can mediate flowering time through their effects on developmental rates of preceding phenophases or by cueing floral development and anthesis. Accordingly, we used mean surface temperatures averaged over a standard period of three months[18,21,53,62] leading up to (and including) the mean flowering month for each species (hereafter 'TMEAN') as a predictor. For each collection site, we obtained monthly TMEAN time series (January 1896 – December 2020) at a 16-km^2 spatial resolution from the Parameter-elevation Regressions on Independent Slopes Model (PRISM Climate Group, Oregon State University, http://prism.oregonstate.edu). We characterized each collection site by its long-term mean temperature (hereafter '$TMEAN_{Normal}$'), averaging observed TMEAN across all years between 1896 and 2020. Annual deviations from long-term TMEAN conditions (hereafter '$TMEAN_{Anomaly}$') at each site and in each year were calculated by subtracting the $TMEAN_{Normal}$ from the observed TMEAN conditions in the year of collection. Positive and negative $TMEAN_{Anomaly}$ values respectively reflect warmer-than-average and colder-than-average years. $TMEAN_{Normal}$ and $TMEAN_{Anomaly}$ were uncorrelated irrespective of the latitudinal and elevational range spanned by a species (median $r = -0.04$), thus representing independent axes of climatic variation (Fig. S2). $TMEAN_{Normal}$ spanned a wider temperature range than $TMEAN_{Anomaly}$ for most species, with respective median ranges of 13.7 °C and 5.4 °C (Fig. S3). Species occurring in cold climates tended to show later mean flowering dates than species occupying warmer regions (Fig. S4a); consequently, average $TMEAN_{Normal}$ values were well above 0°C leading up to the mean flowering dates of all species in our data (Fig. S4b).

To assess how sensitivities varied across climatic gradients (see ***Analyses,*** below), we first characterized long-term precipitation and temperature at each site of collection using a Principal Component Analysis (PCA), with mean annual temperature normal (MAT_{Normal}), mean annual precipitation normal (PPT_{Normal}), temperature seasonality, and precipitation seasonality as input features. We obtained precipitation (hereafter 'PPT') data from PRISM and calculated PPT and temperature seasonality for each collection site as the difference between the months with the highest and lowest PPT and mean temperature normal, respectively. We made PPT seasonality proportional to local levels of precipitation by dividing differences in maximum versus minimum monthly precipitation normal by PPT_{Normal} at each site. The PCA identified 2 principal components accounting for more variance than its input features, jointly explaining 78% of observed variation. PC1 was associated with increasing PPT seasonality (36%), decreasing temperature seasonality (31%) and increasing MAT_{Normal} (28%) (Extended Data Fig. 2). PC2 represented a gradient of decreasing PPT_{Normal} (74%) and increasing temperature seasonality (22%).

Analyses

Estimating apparent plasticity and adaptation—We estimated flowering time sensitivity to $TMEAN_{Normal}$ and $TMEAN_{Anomaly}$ using a Bayesian mixed-effects model. The model fitted species-specific intercepts and slopes and treated them as random effects sampled from 'community-level' distributions (defined by among-species mean and standard deviation of intercepts and slopes). This hierarchical structure improved estimation of parameters by using information and estimates from all species in the data. In turn, the Bayesian inference framework allowed for estimation of the correlations between TMEAN sensitivities over space and time and their differences for each species while propagating parameter uncertainty.

We used DOY for each observation *i* as a response, assuming a normal distribution with mean μ_i and species-specific standard deviation σ_{sp}:

$$DOY_i \sim N(\mu_i, \sigma_{sp}) \tag{1}$$

We modeled μ_i as a linear function of $TMEAN_{Normal}$ (TMEAN $Norm_i$), and $TMEAN_{Anomaly}$ (TMEAN $Anom_i$) for each observation *i*.

$$\mu_i = \alpha_{sp} + S_{space_{sp}} \times TMEAN\ Norm_i + S_{time_{sp}} \times TMEAN\ Anom_i \tag{2}$$

For each species *sp*, the model yielded intercepts representing mean flowering dates (α_{sp}), sensitivities (i.e., regression slopes) for TMEAN normal ($S_{space_{sp}}$), and sensitivities for TMEAN anomaly ($S_{time_{sp}}$).

To assess the correlation between S_{space} and S_{time}, we modeled community-level distributions for intercepts and slopes as generated by a multivariate normal distribution with a vector of hypermeans μ and a variance-covariance matrix Σ:

$$\left(\alpha_{sp}, S_{N_{sp}}, S_{A_{sp}}\right) \sim N(\mu, \Sigma) \quad (3)$$

We also calculated the difference between sensitivity types ($S_{space_{sp}} - S_{time_{sp}}$) as a derived quantity within the model, which we interpreted as the degree of apparent local adaptation in DOY observed across the TMEAN normal gradient (Fig. 1), with negative and positive values respectively indicating advances and delays in flowering DOY across warmer locations.

We used weakly informative priors, with wide, 0-centered normal distributions for intercepts, slopes, and rate parameters for exponential distributions (used to obtain species-specific variances). For the variance-covariance matrix **Σ,** we used a Lewandowski-Kurowicka-Joe (LKJ) Cholesky covariance prior, with $\eta = 1$ to allow for high correlations among parameters. Posterior distributions were obtained using Hamiltonian Monte Carlo (HMC) in Stan (code provided in Note S2) as implemented in R v.4.2.1 using the 'rstan' package v.2.21.2[63]. We implemented a non-centered parameterization to improve sampling of the parameter space. Sampling was done using three MCMC chains with a training period of 1000 iterations and sampling of 4000 iterations. All S_{space}, S_{time}, and $S_{space} - S_{time}$ estimates had Gelman-Rubin statistics ('R-hat') of less than 1.002, and visual examination of trace plots confirmed convergence.

Fitting the model on simulated data (Note S3), which emulated the average range of TMEAN conditions and the signal-to-noise ratio of DOY vs. TMEAN observed within species in our data, confirmed that our model could accurately recover the parameters of interest (S_{time}, S_{space}, and $S_{space} - S_{time}$) for a range of sample and effect sizes (Note S3; Figs. S5–7). Moreover, we found that apparent plasticity (S_{time}) and apparent adaptation ($S_{space} - S_{time}$) could be estimated with similar degrees of precision (Fig. S8).

Because our model did not include an explicit temporal predictor, it may appear to ignore widespread trends in phenology and temperature reported in recent decades. However, additional simulation analyses (Note S4) showed that our model does account for temporal trends in phenology among species that experience trends in $TMEAN_{Anomaly}$ over time and that are responsive to $TMEAN_{Anomaly}$ (i.e., non-zero S_{time}) (Fig. S9a). To evaluate the model's implicit assumption that trends in $TMEAN_{Anomaly}$ cause observed trends in phenology, we used the herbarium dataset to determine empirically whether observed temporal trends in $TMEAN_{Anomaly}$ and a species' S_{time} indeed explain observed trends in DOY. We recovered the same patterns observed in the simulation (Fig. S9b), suggesting that phenology and $TMEAN_{Anomaly}$ trends are causally related. Moreover, detrending DOY and $TMEAN_{Anomaly}$ prior to fitting the model did not affect our results, suggesting that omitting time as a covariate was unlikely to bias our results (Extended Data Fig. 3).

Finally, we evaluated the impact on our estimates of choosing alternative reference periods to calculate $TMEAN_{Normal}$ (i.e., 1901–2020 vs. 1901–1930, 1931–1960, 1961–1990, 1991–2020) (Note S5, Figs. S10–12). These analyses confirmed that period selection was unlikely to have affected our results.

Exploring assumptions—Herbarium specimens rarely are collected repeatedly at the same location across years. Accordingly, we found few repeated collections over time and in close enough proximity to represent single populations. Because of this, we estimated S_{space} and S_{time} using statistical methods different from Phillimore et al.[9] and Delgado et al.[23] (Note S6). Nevertheless, the interpretation of our model relied on the same simplifying assumptions: spatial slopes reflect variation in DOY among populations along a temperature gradient, temporal slopes reflect plasticity, plasticity does not vary within and among populations, and the temporal and spatial relationships between phenology and climate are not biased by confounding factors.

We evaluated the plausibility of many of these assumptions. S_{space} likely represented phenological variation among populations because conspecific specimens were collected over vast regions spanning median latitudinal and longitudinal ranges of 1,356 km and 1,819 km (removing outliers), respectively. In turn, S_{time} likely reflected the effects of plasticity and not adaptation: analyses including only long-lived perennials (unlikely to show microevolutionary changes over short periods) yielded very similar results to those presented below (Extended Data Fig. 1); moreover, detrending DOY and $TMEAN_{Anomaly}$ prior to fitting the model—which may account for temporal confounds or microevolution[64]—yielded nearly identical estimates (Extended Data Fig. 3). Furthermore, we generated a single estimate of S_{time} per species, thus assuming uniform plastic responses within and among populations. This assumption was supported by the observation that, for a large majority of species, S_{time} did not vary along geographic gradients of long-term TMEAN, long-term PPT, TMEAN seasonality, PPT seasonality, or the joint gradients described by PC1 and PC2 (Extended Data Fig. 4). Cumulative precipitation and photoperiod are unlikely to confound S_{space} and S_{time}: accounting for cumulative PPT yielded nearly identical estimates in single-species models (Extended Data Fig. 5), and an analysis of 120 species collected withing geographic ranges restricted to narrower latitudinal bands (≤1°)—and therefore to limited geographically-driven variation in photoperiod—yielded results very similar to those based on the entire dataset (Extended Data Fig. 6). Finally, we detected no biases in S_{space} or S_{time} due to differences in sample size among species (Extended Data Figs. 7a, b), phylogeny (Extended Data Figs. 7c, d), spatial autocorrelation (Extended Data Figs. 7e, f), non-linear phenology-temperature relationships (Extended Data Fig. 8), or difference in range size among species (Extended Data Fig. 9).

Although herbarium data has many spatial and temporal collection biases and limitations—including preferential collection near roads and urban areas, and sharp decreases in collection intensity in recent decades[65]—such biases are likely not severe in our data (Notes S7, 8, Figs. S13–20). Our estimates of S_{space}, S_{time}, and $S_{space} – S_{time}$ were robust to inclusion in our models of factors such as urbanization (Fig. S14) and proximity to major roads (Figs. S17, 18), and showed no evidence of various forms of temporal non-independence (Fig. S20). Collector preferences can result in overrepresentation of certain taxa or traits among specimens[65]. While we cannot rule out these biases in our data, our study encompassed species from 106 families and 740 genera, capturing vast functional, evolutionary, and life history diversity. Therefore, we consider it unlikely that our results were driven by overrepresentation of taxa or traits. Finally, some herbaria obscure location data for endangered or heavily poached species. However, since we only included georeferenced specimens from well-represented species—of which only 12 (0.7% of the total) are listed as endangered by the United States Department of Agriculture[66]—it is unlikely that our species list includes many such taxa.

Categorizing sensitivity patterns—To assess the prevalence of apparent plasticity and adaptation among species, we categorized each species' S_{space} versus S_{time} patterns as consistent with the effects of plasticity alone (Figs. 1a,b), adaptation alone (Figs. 1c,d), the joint effects of plasticity and adaptation (co- or counter-gradient adaptation; Figs. 1e–h), or neither. Classifications were based on the proportion of the posterior probability distribution of S_{time} and $S_{space} - S_{time}$ lying in the direction of their *maximum a posteriori* (MAP) estimate (i.e., their "probability of direction", henceforth 'PD'). PD is bound by 0.5 (maximum uncertainty about the effect of the predictor) and 1 (certainty of an effect in the direction of the MAP estimate). We subjectively considered apparent plasticity (S_{time}) and adaptation ($S_{space} - S_{time}$) as significant when their PD was ≥ 0.95 (Table 1). Apparent plasticity and adaptation showed similar levels of estimation uncertainty both empirically (SD = 0.87 ± 0.34 d/°C for S_{time}; SD = 0.93 ± 0.32 d/°C for $S_{space} - S_{time}$) and in simulation analyses (Note S3), suggesting sensitivity patterns were not substantially more likely to be classified as consistent with plasticity than with adaptation (and vice versa) due to estimation uncertainty.

Phenological niches, local climates, and ecoregions—To assess how apparent plasticity and adaptation varied with native climate and phenological niche among species, we first calculated the mean flowering DOY and the mean coordinates along the climate gradients described by PC1 and PC2 among specimens of each species. We then fit two generalized additive models (GAMs) using S_{time} or $S_{space} - S_{time}$ as responses—assumed to be normally distributed—and a three-variable tensor-product smooth of mean flowering DOY, mean PC1, and mean PC2 as a predictor. This design allowed us to assess how native climate and phenological niche jointly determined the apparent roles of plasticity and adaptation while accounting for possible interactions and non-linearities. Because S_{time} and $S_{space} - S_{time}$ are estimates, we accounted for parameter uncertainty by weighting each observation by the inverse of its posterior variance (i.e., its precision).

Additionally, we assessed the relative contributions of apparent plasticity and adaptation throughout the season within ecoregions of the contiguous United States. To do so, we identified the Level II Ecoregion—as classified by the USA Environmental Protection Agency (EPA)[67,68]—within which each specimen was collected. We used Level II Ecoregions because they provide sufficient ecological detail to distinguish regional floras while encompassing areas broad enough for each to capture multiple species in our data. To avoid inflating species overlap among regions or the influence of species that were rarely sampled within an ecoregion, we arbitrarily considered a species as present within an ecoregion if at least 10% of its collections occurred within it. We then retained only ecoregions represented by a minimum of 8 species. Under this scheme, the median species was classified as occurring within 2 ecoregions (range =

1–7), the median ecoregion was represented by 156 species (range = 17–956 for Atlantic Highlands and Western Cordilleras, respectively), and pairs of ecoregions shared, on average, 4% of their species (range = 0–39%; Fig. S21). Of the 120 ecoregion pairs examined, 57 shared less than 1% of species, 100 shared less than 10% of species, and 114 shared less than 20% of species.

Once species × ecoregion combinations were identified (n = 3,570), we fitted two GAMs including apparent plasticity (S_{time}) or apparent adaptation ($S_{space} - S_{time}$) as a response, ecoregion as a categorical predictor, mean flowering DOY as continuous predictor, and a mean flowering DOY × ecoregion spline assessing the ecoregion-specific effects of mean DOY on apparent plasticity or adaptation. Again, we accounted for parameter uncertainty by weighting each observation by the precision of its corresponding apparent plasticity or adaptation estimate. Collection locations in different ecoregions differed substantially in their long-term climatic conditions (Extended Data Fig. 10). However, we assumed no intraspecific variation in S_{time} across ecoregions an assumption partially supported by the observation that S_{time} did not tend to vary along climatic gradients within species (Extended Data Fig. 4). All GAMs were implemented using the 'mgcv' package v.1.8-40 in R[69,70].

Data availability

The data used in this study are publicly available on Zenodo[6]

Code Availability

All code necessary to reproduce the main results, extended data figures, and supplements is available on Zenodo[61].

Acknowledgments

This work was supported by the National Science Foundation through NSF DEB-1556768 (to S.J.M., I.W.P.), NSF DEB-2105932 (to S.J.M., I.W.P), NSF DEB-2105907 (to S.R.) and NSF DEB-2105903 (to C.C.D.). T.R.P is grateful to UCSB for fellowship support in the year this manuscript was completed. We thank the many herbaria, including botanists, staff and volunteers, who collected, curated, and digitized the vast volumes of herbarium specimens leveraged for this study. We thank Ann Bishop, Devin Gamble, Cameron Hannah-Bick, David Inouye, Lisa Kim, Helen Payne for comments on earlier drafts of the manuscript.

Author contributions

T.R.P. conceived the initial ideas, which were further developed and refined with S.J.M and I.W.P.; I.W.P collected the data; T.R.P. designed and conducted the data analyses and created the figures; T.R.P. wrote the first draft, and all authors contributed significantly to subsequent revisions.

Competing interests

The authors declare no competing interests.

TABLES

Biological Process		Empirical Sensitivity Pattern
Plasticity only		1. Probability of direction for $S_{time} \geq 0.95$ 2. Probability of direction for $S_{space} - S_{time} < 0.95$
Adaptation only		1. Probability of direction for $S_{space} - S_{time} \geq 0.95$ 2. Probability of direction for $S_{time} < 0.95$
Plasticity and Adaptation	*Co-gradient*	1. Probability of direction for $S_{time} \geq 0.95$ 2. Probability of direction for $S_{space} - S_{time} \geq 0.95$ 3. S_{space} and S_{time} have the same direction 4. $\lvert S_{space} \rvert > \lvert S_{time} \rvert$
	Counter-gradient	1. Probability of direction for $S_{time} \geq 0.95$ 2. Probability of direction for $S_{space} - S_{time} \geq 0.95$ **Case 1:** 3. S_{space} and S_{time} have opposite direction **Case 2:** 4. S_{space} and S_{time} have the same direction 5. $\lvert S_{space} \rvert < \lvert S_{time} \rvert$
Neither		1. Probability of direction for $S_{time} < 0.95$ 2. Probability of direction for $S_{space} - S_{time} < 0.95$

Table 1—Criteria for classifying the sensitivity pattern of each species. Patterns were classified as consistent with the role of plasticity only, adaptation only, the joint effects of plasticity and adaptation in a co- or counter-gradient adaptation pattern, or neither adaptation nor plasticity. The probability that S_{time} or $S_{space} - S_{time}$ differed from 0 in the direction of its maximum a posteriori (MAP) estimate (i.e., their probability of direction) was obtained from the posterior distribution of these parameters for each species.

FIGURE LEGENDS

Figure 1—Spatial and temporal relationships between flowering time and temperature resulting from plasticity and adaptation. (**a**) Local adaptation acting as the sole driver of flowering time along the gradient (i.e., no phenological plasticity) should result in (**b**) a negligible temporal relationship and a biologically significant difference between temporal and spatial slopes. In contrast, (**c**) plasticity acting as the sole driver of flowering time variation along the gradient (i.e., no adaptation) should result in (**d**) a biologically significant temporal relationship and negligible differences between spatial and temporal slopes. Local adaptation and plasticity jointly influencing flowering time should result in different empirical patterns depending on the direction of their effects. (**e**) Plasticity and adaptation operating in the same direction (e.g., both negative) should result in (**f**) a biologically significant temporal relationship and a spatial relationship of significantly greater magnitude. In contrast, (**g**) plasticity and adaptation operating in opposite directions (e.g., plasticity negative, adaptation positive) should result in (**h**) a biologically significant temporal relationship and a spatial relationship of significantly lesser magnitude (or having a different sign altogether). (**i**) Species exhibiting no plasticity or adaptation along the gradient would generate (**j**) biologically non-significant temporal and spatial slopes. Orange lines in **a**, **c**, **e**, and **g** illustrate phenological responses of spatially separated populations to temporal temperature variation, which spans a narrower temperature range than spatial temperature variation across the entire species range (segmented red lines). The biological processes in **a, c, e**, and **g** generate the empirical patterns in **b, d, f**, and **h**. In turn, the empirical patterns imply the processes that generated them. See "**Methods** – *Exploring Assumptions*" for an overview of the assumptions of this approach and the degree to which they were met by our data. For examples of species exhibiting each of these patterns, see Fig. S1.

Figure 2—Distributions of, and relationship between S_{space} and S_{time} among 1,605 North American angiosperms. Shaded regions in (**a**) correspond to the kernel density distributions of S_{time} (red) and S_{space} (blue) among species. Each point in (**b**) represents a species whose *x, y* coordinates are given by the maximum a posteriori (MAP) estimates for S_{space} and S_{time}, respectively. Colors in (**b**) indicate whether sensitivity patterns were consistent with plasticity

(green) or adaptation (magenta) as the sole drivers of flowering time variation along the temperature gradient, with both plasticity and adaptation in a co- or counter-gradient adaptation pattern (blue, orange), or neither (dark yellow). The straight, solid black line in (**b**) indicates a 1:1 relationship (i.e., $S_{space} = S_{time}$), whereas the curved solid line shows the observed relationship estimated from a generalized additive model (GAM). The shaded region along the curved solid line in (b) corresponds to the standard error of the predicted value of S_{time}. The percent of species showing each pattern is shown in parentheses in the legend. The 95% credible interval for the correlation between S_{space} and S_{time} is provided as a text inset in (**b**).

Figure 3—Variation in apparent plasticity (S_{time}) and apparent adaptation ($S_{space} - S_{time}$) attributable to differences in phenological niche and native climate among species. PC1 (**a**, **b**) represents a climate gradient of increasing precipitation seasonality, decreasing temperature seasonality, and increasing mean annual temperature, whereas PC2 (**c, d**) corresponds to a gradient of decreasing mean annual precipitation and increasing temperature seasonality. The color gradients in each panel represents the predicted magnitude of S_{time} or $S_{space} - S_{time}$ (in days/°C) for a combination of mean flowering DOY and PC1 or PC2 values. The predicted surfaces represented by the color gradients were obtained using three-variable tensor smooths in a generalized additive modelling (GAM) framework. In each panel, the value of the third variable (the one not plotted) was fixed at its mean.

Figure 4—Variation in apparent plasticity and apparent adaptation among species with varying phenological niches across ecoregions of the United States. Shaded regions in each panel represent the 95% confidence interval for the mean apparent plasticity or apparent adaptation among species predicted for a given mean flowering date. The predicted mean values for apparent plasticity and adaptation were obtained using generalized additive models (GAMs).

References

1. Elzinga, J. A. *et al.* Time after time: flowering phenology and biotic interactions. *Trends Ecol. Evol.* **22**, 432–439 (2007).
2. Bradshaw, A. D. Evolutionary Significance of Phenotypic Plasticity in Plants. in *Advances in Genetics* (eds. Caspari, E. W. & Thoday, J. M.) vol. 13 115–155 (Academic Press, 1965).
3. Gienapp, P., Teplitsky, C., Alho, J. S., Mills, J. A. & Merilä, J. Climate change and evolution: disentangling environmental and genetic responses. *Mol. Ecol.* **17**, 167–178 (2008).
4. Hoffmann, A. A. & Sgrò, C. M. Climate change and evolutionary adaptation. *Nature* **470**, 479–485 (2011).
5. Franks, S. J., Sim, S. & Weis, A. E. Rapid evolution of flowering time by an annual plant in response to a climate fluctuation. *Proc. Natl. Acad. Sci.* **104**, 1278–1282 (2007).
6. Wu, Y. & Colautti, R. I. Evidence for continent-wide convergent evolution and stasis throughout 150 y of a biological invasion. *Proc. Natl. Acad. Sci.* **119**, e2107584119 (2022).
7. Merilä, J. & Hendry, A. P. Climate change, adaptation, and phenotypic plasticity: the problem and the evidence. *Evol. Appl.* **7**, 1–14 (2014).
8. Fox, R. J., Donelson, J. M., Schunter, C., Ravasi, T. & Gaitán-Espitia, J. D. Beyond buying time: the role of plasticity in phenotypic adaptation to rapid environmental change. *Philos. Trans. R. Soc. B Biol. Sci.* **374**, 20180174 (2019).
9. Phillimore, A. B., Hadfield, J. D., Jones, O. R. & Smithers, R. J. Differences in spawning date between populations of common frog reveal local adaptation. *Proc. Natl. Acad. Sci.* **107**, 8292–8297 (2010).
10. Bonamour, S., Chevin, L.-M., Charmantier, A. & Teplitsky, C. Phenotypic plasticity in response to climate change: the importance of cue variation. *Philos. Trans. R. Soc. B Biol. Sci.* **374**, 20180178 (2019).
11. Ensing, D. J. & Eckert, C. G. Interannual variation in season length is linked to strong co-gradient plasticity of phenology in a montane annual plant. *New Phytol.* **224**, 1184–1200 (2019).
12. Stinchcombe, J. R. *et al.* A latitudinal cline in flowering time in Arabidopsis thaliana modulated by the flowering time gene FRIGIDA. *Proc. Natl. Acad. Sci.* **101**, 4712–4717 (2004).
13. Montague, J. L., Barrett, S. C. H. & Eckert, C. G. Re-establishment of clinal variation in flowering time among introduced populations of purple loosestrife (Lythrum salicaria, Lythraceae). *J. Evol. Biol.* **21**, 234–245 (2008).

14. Anderson, J. T., Inouye, D. W., McKinney, A. M., Colautti, R. I. & Mitchell-Olds, T. Phenotypic plasticity and adaptive evolution contribute to advancing flowering phenology in response to climate change. *Proc. R. Soc. B Biol. Sci.* **279**, 3843–3852 (2012).
15. Conover, D. O. & Schultz, E. T. Phenotypic similarity and the evolutionary significance of countergradient variation. *Trends Ecol. Evol.* **10**, 248–252 (1995).
16. Nylin, S. & Gotthard, K. Plasticity in Life-History Traits. *Annu. Rev. Entomol.* **43**, 63–83 (1998).
17. Fitter, A. H. & Fitter, R. S. R. Rapid Changes in Flowering Time in British Plants. *Science* **296**, 1689–1691 (2002).
18. Cook, B. I. *et al.* Sensitivity of Spring Phenology to Warming Across Temporal and Spatial Climate Gradients in Two Independent Databases. *Ecosystems* **15**, 1283–1294 (2012).
19. Lapenis, A., Henry, H., Vuille, M. & Mower, J. Climatic factors controlling plant sensitivity to warming. *Clim. Change* **122**, 723–734 (2014).
20. Zhang, H., Yuan, W., Liu, S., Dong, W. & Fu, Y. Sensitivity of flowering phenology to changing temperature in China. *J. Geophys. Res. Biogeosciences* **120**, 1658–1665 (2015).
21. Park, D. S. *et al.* Herbarium specimens reveal substantial and unexpected variation in phenological sensitivity across the eastern United States. *Philos. Trans. R. Soc. B Biol. Sci.* **374**, 20170394 (2019).
22. Prevéy, J. S. *et al.* Warming shortens flowering seasons of tundra plant communities. *Nat. Ecol. Evol.* **3**, 45–52 (2019).
23. Delgado, M. del M. *et al.* Differences in spatial versus temporal reaction norms for spring and autumn phenological events. *Proc. Natl. Acad. Sci.* **117**, 31249–31258 (2020).
24. Li, D. *et al.* Climate, urbanization, and species traits interactively drive flowering duration. *Glob. Change Biol.* **27**, 892–903 (2021).
25. Davis, C. C., Willis, C. G., Connolly, B., Kelly, C. & Ellison, A. M. Herbarium records are reliable sources of phenological change driven by climate and provide novel insights into species' phenological cueing mechanisms. *Am. J. Bot.* **102**, 1599–1609 (2015).
26. Willis, C. G. *et al.* Old Plants, New Tricks: Phenological Research Using Herbarium Specimens. *Trends Ecol. Evol.* **32**, 531–546 (2017).
27. Park, D. S., Breckheimer, I. K., Ellison, A. M., Lyra, G. M. & Davis, C. C. Phenological displacement is uncommon among sympatric angiosperms. *New Phytol.* **233**, 1466–1478 (2022).
28. Ramirez-Parada, T. H., Park, I. W. & Mazer, S. J. Herbarium specimens provide reliable estimates of phenological responses to climate at unparalleled taxonomic and spatiotemporal scales. Ecography 2022, e06173 (2022).29.

29. Park, I. W. & Mazer, S. J. Overlooked climate parameters best predict flowering onset: Assessing phenological models using the elastic net. *Glob. Change Biol.* **24**, 5972–5984 (2018).
30. Park, I. W., Ramirez-Parada, T. & Mazer, S. J. Advancing frost dates have reduced frost risk among most North American angiosperms since 1980. *Glob. Change Biol.* **27**, 165–176 (2021).
31. Kharouba, H. M. & Vellend, M. Flowering time of butterfly nectar food plants is more sensitive to temperature than the timing of butterfly adult flight. *J. Anim. Ecol.* **84**, 1311–1321 (2015).
32. Munson, S. M. & Long, A. L. Climate drives shifts in grass reproductive phenology across the western USA. *New Phytol.* **213**, 1945–1955 (2017).
33. Kopp, C. W., Neto-Bradley, B. M., Lipsen, L. P. J., Sandhar, J. & Smith, S. Herbarium records indicate variation in bloom-time sensitivity to temperature across a geographically diverse region. *Int. J. Biometeorol.* (2020) doi:10.1007/s00484-020-01877-1.
34. Pearson, K. D., Love, N. L. R., Ramirez-Parada, T., Mazer, S. J. & Yost, J. M. Phenological trends in the California poppy (Eschscholzia californica): digitized specimens reveal intraspecific variation in the sensitivity of flowering date to Climate Change. *Madroño* **68**, 343–359 (2021).
35. Mazer, S. J., Love, N. L. R., Park, I. W., Ramirez-Parada, T. & Matthews, E. R. Phenological sensitivities in two Clarkia congeners: indirect evidence for facilitation, convergence, niche conservatism, or genetic constraints. *Madroño* **68**, 388–405 (2021).
36. Park, D. S., Xie, Y., Ellison, A. M., Lyra, G. M. & Davis, C. C. Complex climate-mediated effects of urbanization on plant reproductive phenology and frost risk. *New Phytol.* **n/a**, (2023).
37. Kramer, K. Phenotypic plasticity of the phenology of seven European tree species in relation to climatic warming. *Plant Cell Environ.* **18**, 93–104 (1995).
38. Levin, D. A. Flowering-time plasticity facilitates niche shifts in adjacent populations. *New Phytol.* **183**, 661–666 (2009).
39. De FRENNE, P. *et al.* Temperature effects on forest herbs assessed by warming and transplant experiments along a latitudinal gradient. *Glob. Change Biol.* **17**, 3240–3253 (2011).
40. Franks, S. J., Weber, J. J. & Aitken, S. N. Evolutionary and plastic responses to climate change in terrestrial plant populations. *Evol. Appl.* **7**, 123–139 (2014).
41. Vitasse, Y. *et al.* Elevational adaptation and plasticity in seedling phenology of temperate deciduous tree species. *Oecologia* **171**, 663–678 (2013).
42. Colautti, R. I. & Barrett, S. C. H. Rapid Adaptation to Climate Facilitates Range Expansion of an Invasive Plant. *Science* **342**, 364–366 (2013).
43. Ackerly, D. D. *et al.* Topoclimates, refugia, and biotic responses to climate change. *Front. Ecol. Environ.* **18**, 288–297 (2020).

44. Wolkovich, E. M., Cook, B. I. & Davies, T. J. Progress towards an interdisciplinary science of plant phenology: building predictions across space, time and species diversity. *New Phytol.* **201**, 1156–1162 (2014).
45. Chown, S. *et al.* Adapting to climate change: a perspective from evolutionary physiology. *Clim. Res.* **43**, 3–15 (2010).
46. Fu, Y. H. *et al.* Declining global warming effects on the phenology of spring leaf unfolding. *Nature* **526**, 104–107 (2015).
47. Güsewell, S., Furrer, R., Gehrig, R. & Pietragalla, B. Changes in temperature sensitivity of spring phenology with recent climate warming in Switzerland are related to shifts of the preseason. *Glob. Change Biol.* **23**, 5189–5202 (2017).
48. Wolkovich, E. M., Chamberlain, C. J., Buonaiuto, D. M., Ettinger, A. K. & Morales-Castilla, I. Integrating experiments to predict interactive cue effects on spring phenology with warming. *New Phytol.* **235**, 1719–1728 (2022).
49. Iler, A. M., CaraDonna, P. J., Forrest, J. R. K. & Post, E. Demographic Consequences of Phenological Shifts in Response to Climate Change. *Annu. Rev. Ecol. Evol. Syst.* **52**, annurev-ecolsys-011921-032939 (2021).
50. De Lisle, S. P., Mäenpää, M. I. & Svensson, E. I. Phenotypic plasticity is aligned with phenological adaptation on both micro- and macroevolutionary timescales. *Ecol. Lett.* **25**, 790–801 (2022).
51. Amasino, R. Seasonal and developmental timing of flowering. *Plant J.* **61**, 1001–1013 (2010).
52. Wolkovich, E. M. *et al.* Warming experiments underpredict plant phenological responses to climate change. *Nature* **485**, 494–497 (2012).
53. Mazer, S. J. *et al.* Flowering date of taxonomic families predicts phenological sensitivity to temperature: Implications for forecasting the effects of climate change on unstudied taxa. *Am. J. Bot.* **100**, 1381–1397 (2013).
54. 1. Beil, I., Kreyling, J., Meyer, C., Lemcke, N. & Malyshev, A. V. Late to bed, late to rise—Warmer autumn temperatures delay spring phenology by delaying dormancy. Global Change Biology 27, 5806–5817 (2021).
55. Zhou, Z. *et al.* Lengthened flowering season under climate warming: Evidence from manipulative experiments. *Agric. For. Meteorol.* **312**, 108713 (2022).
56. Roslin, T. *et al.* Phenological shifts of abiotic events, producers and consumers across a continent. *Nat. Clim. Change* 1–8 (2021) doi:10.1038/s41558-020-00967-7.
57. Sherry, R. A. *et al.* Divergence of reproductive phenology under climate warming. *Proc. Natl. Acad. Sci.* **104**, 198–202 (2007).

58. Chen, L. *et al.* Leaf senescence exhibits stronger climatic responses during warm than during cold autumns. *Nat. Clim. Change* **10**, 777–780 (2020).
59. Zohner, C. M. *et al.* Effect of climate warming on the timing of autumn leaf senescence reverses after the summer solstice. *Science* **381**, eadf5098 (2023).
60. Boyle, B. *et al.* The taxonomic name resolution service: an online tool for automated standardization of plant names. *BMC Bioinformatics* **14**, 16 (2013).
61. Ramirez-Parada, T. H. et al. Data and Code for: Plasticity and not adaptation is the primary source of temperature-mediated variation in flowering phenology in North America (Version 0) [Data set]. Zenodo (2023). https://doi.org/10.5281/zenodo.8310387.
62. Calinger, K. M., Queenborough, S. & Curtis, P. S. Herbarium specimens reveal the footprint of climate change on flowering trends across north-central North America. *Ecol. Lett.* **16**, 1037–1044 (2013).
63. Carpenter, B. *et al. Stan*: A Probabilistic Programming Language. *J. Stat. Softw.* **76**, (2017).
64. Iler, A. M., Inouye, D. W., Schmidt, N. M. & Høye, T. T. Detrending phenological time series improves climate–phenology analyses and reveals evidence of plasticity. *Ecology* **98**, 647–655 (2017).
65. Daru, B. H. *et al.* Widespread sampling biases in herbaria revealed from large-scale digitization. *New Phytol.* **217**, 939–955 (2018).
66. USDA, NRCS, N. P. D. T. The PLANTS Database (http://plants.usda.gov, 08/23/2023). (2023).
67. Omernik, J. M. Ecoregions of the Conterminous United States. *Ann. Assoc. Am. Geogr.* **77**, 118–125 (1987).
68. Omernik, J. M. & Griffith, G. E. Ecoregions of the Conterminous United States: Evolution of a Hierarchical Spatial Framework. *Environ. Manage.* **54**, 1249–1266 (2014).
69. Wood, S. N. Generalized additive models: an introduction with R. *CRC Press/Taylor & Francis Group* (2017).
70. R Core Team. R: A language and environment for statistical computing. (2013).
71. Jin, Y. & Qian, H. V.PhyloMaker: an R package that can generate very large phylogenies for vascular plants. *Ecography* **42**, 1353–1359 (2019).
72. Paradis, E., Claude, J., & Strimmer, K. (2004). APE: analyses of phylogenetics and evolution in R language. *Bioinformatics*, **20(2)**, 289-290
73. Bürkner, P. C. (2017). brms: An R package for Bayesian multilevel models using Stan. *Journal of statistical software*, **80**, 1-28.
74. Pinheiro, J., Bates, D., DebRoy, S., Sarkar, D., Heisterkamp, S., Van Willigen, B., & Maintainer, R. (2017). Package 'nlme'. Linear and nonlinear mixed effects models, version, 3(1).

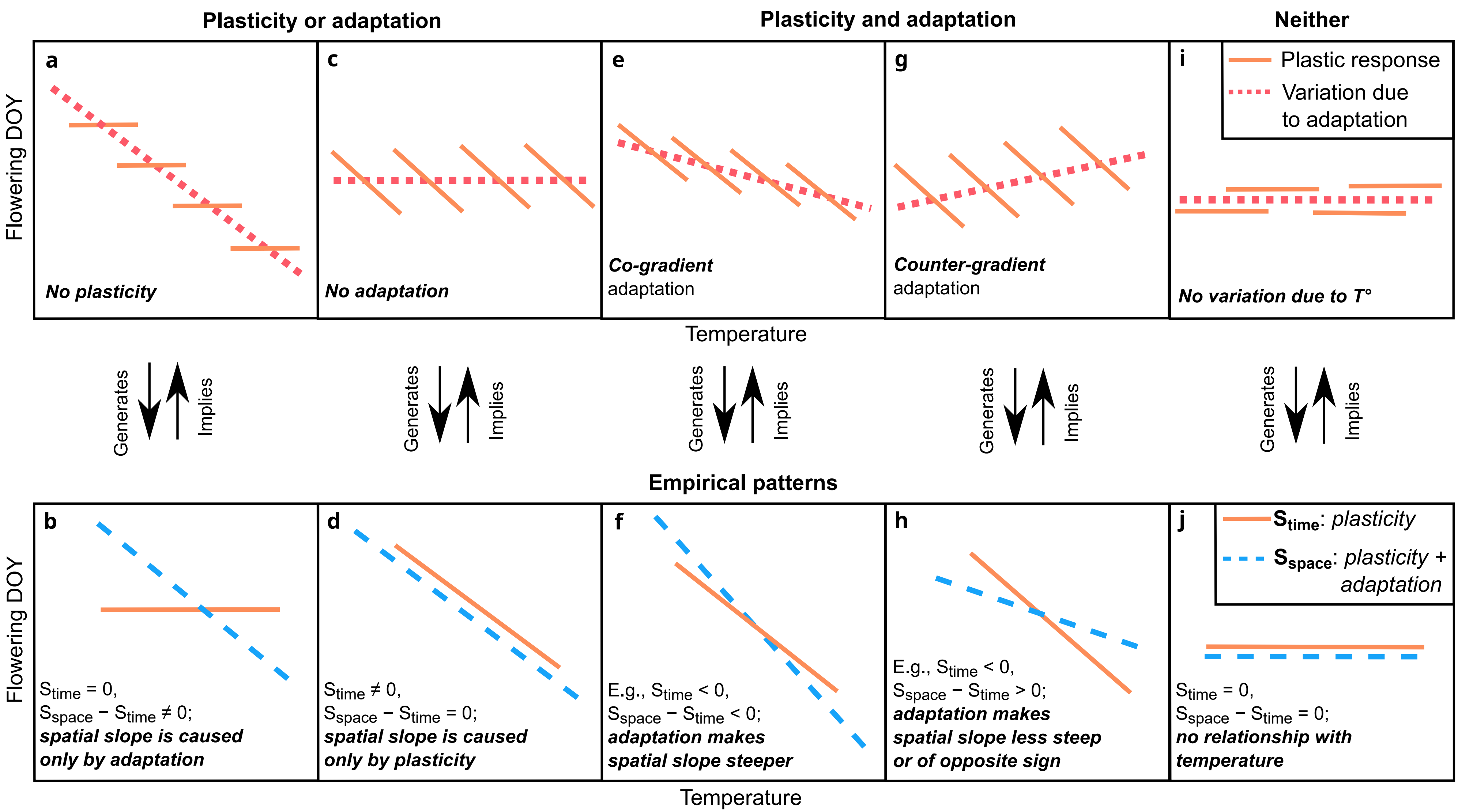

Plasticity or adaptation
Plasticity and adaptation
Neither
Flowering DOY
a
No plasticity
c
No adaptation
e
Co-gradient
adaptation
g
Counter-gradient
adaptation
i
Plastic response
Variation due to adaptation
No variation due to T°
Temperature
Generates
Implies
Empirical patterns
b
$S_{time} = 0$,
$S_{space} - S_{time} \neq 0$;
spatial slope is caused only by adaptation
d
$S_{time} \neq 0$,
$S_{space} - S_{time} = 0$;
spatial slope is caused only by plasticity
f
E.g., $S_{time} < 0$,
$S_{space} - S_{time} < 0$;
adaptation makes spatial slope steeper
h
E.g., $S_{time} < 0$,
$S_{space} - S_{time} > 0$;
adaptation makes spatial slope less steep or of opposite sign
j
S_{time}: plasticity
S_{space}: plasticity + adaptation
$S_{time} = 0$,
$S_{space} - S_{time} = 0$;
no relationship with temperature
Temperature

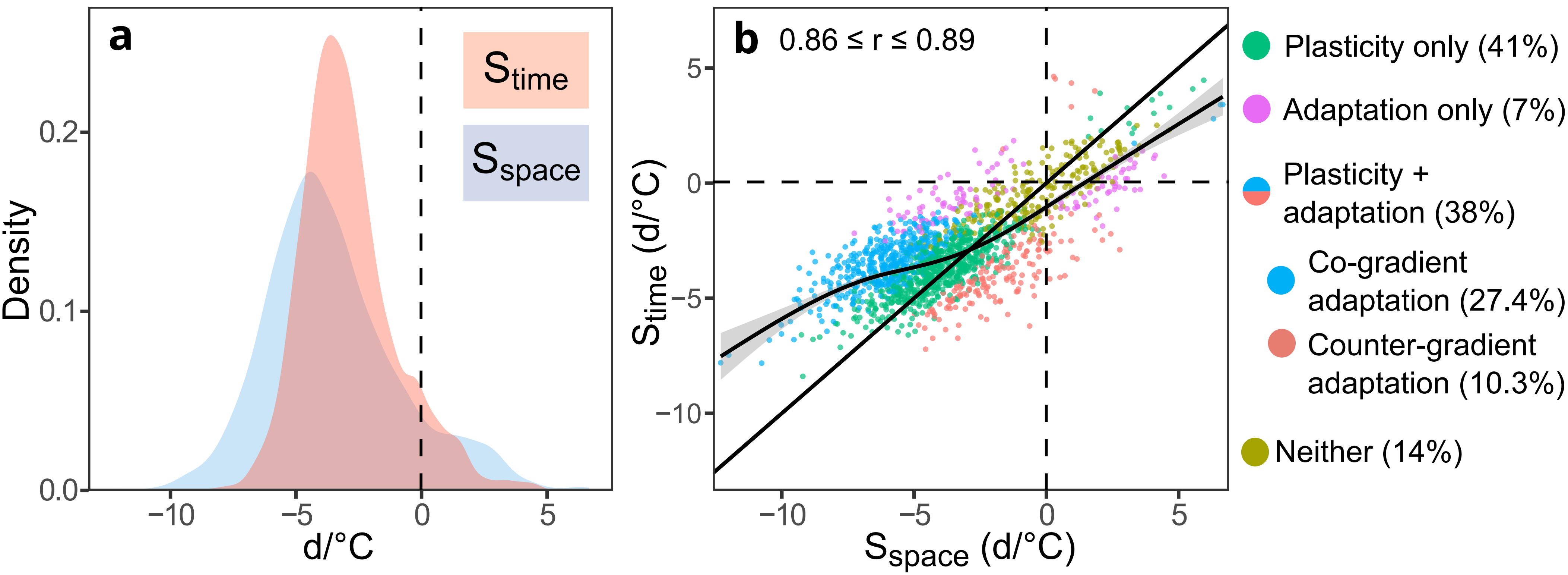

a
Density
0.2
0.1
0.0
−10
−5
0
5
d/°C
S time
S space
b
0.86 ≤ r ≤ 0.89
S time (d/°C)
5
0
−5
−10
S space (d/°C)
Plasticity only (41%)
Adaptation only (7%)
Plasticity + adaptation (38%)
Co-gradient adaptation (27.4%)
Counter-gradient adaptation (10.3%)
Neither (14%)

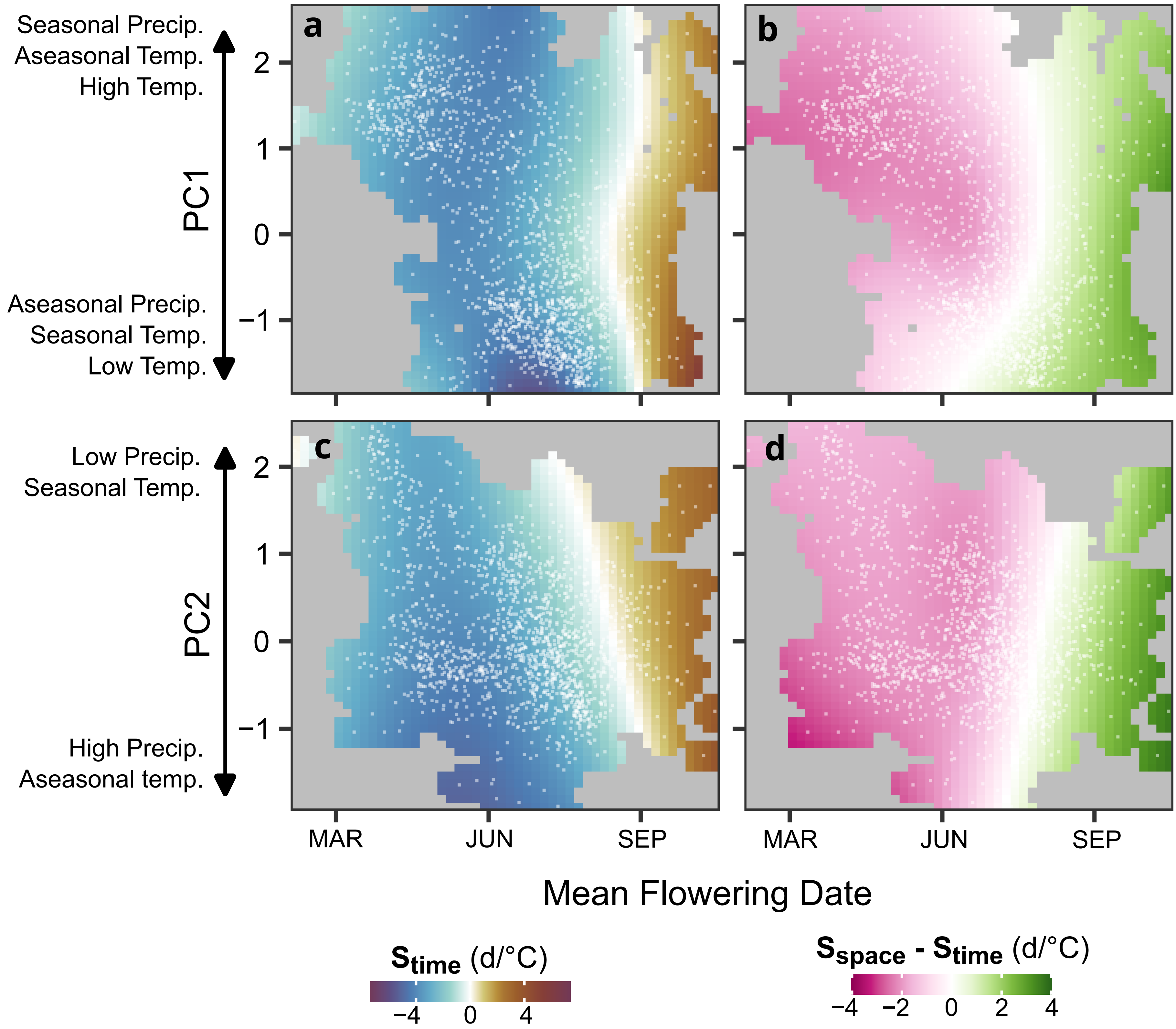

a
b
c
d
Seasonal Precip.
Aseasonal Temp.
High Temp.
Aseasonal Precip.
Seasonal Temp.
Low Temp.
PC1
Low Precip.
Seasonal Temp.
High Precip.
Aseasonal temp.
PC2
2
1
0
−1
MAR
JUN
SEP
Mean Flowering Date
Stime (d/°C)
−4
0
4
Sspace - Stime (d/°C)
−4
−2
0
2
4

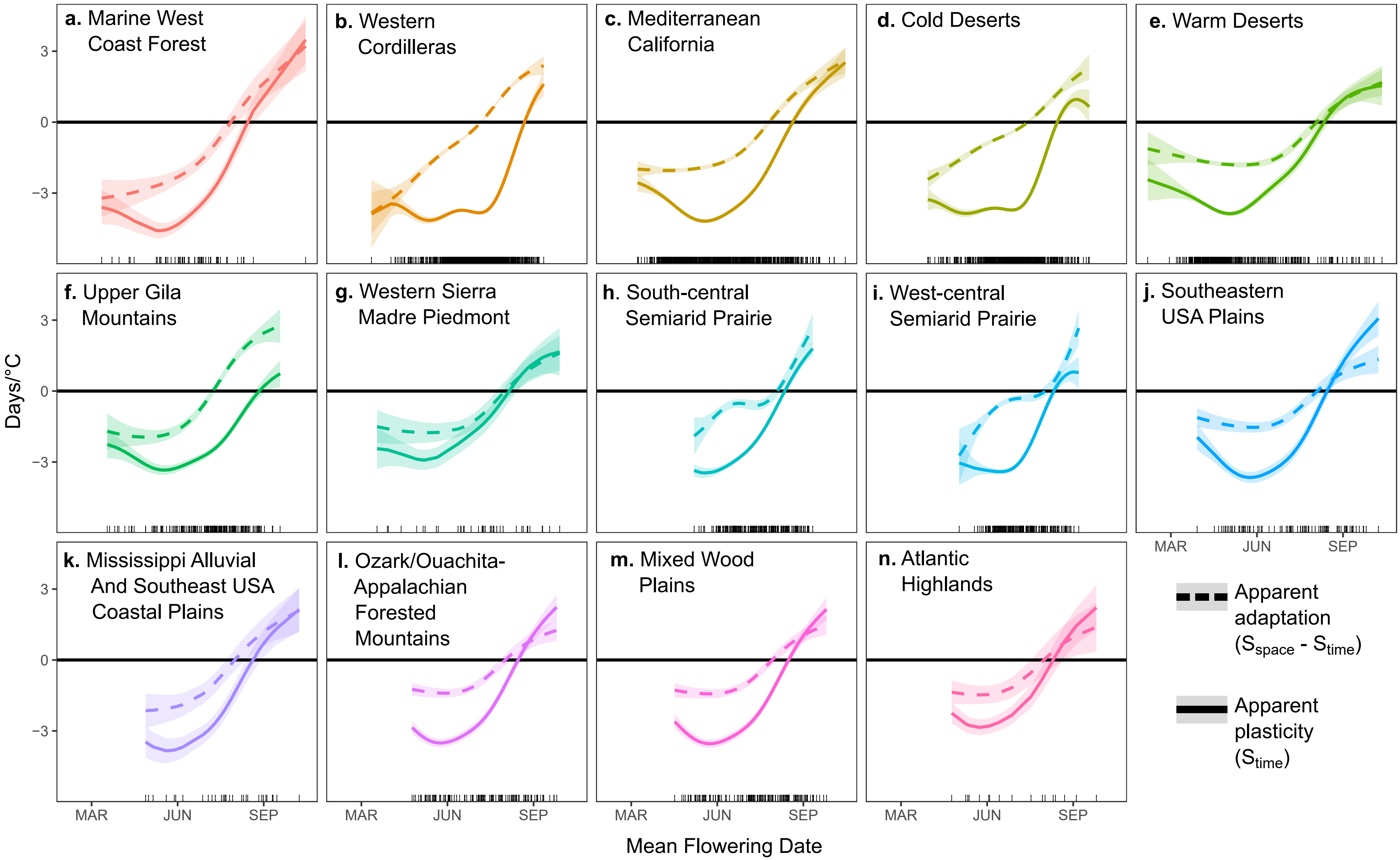

a. Marine West Coast Forest
b. Western Cordilleras
c. Mediterranean California
d. Cold Deserts
e. Warm Deserts
f. Upper Gila Mountains
g. Western Sierra Madre Piedmont
h. South-central Semiarid Prairie
i. West-central Semiarid Prairie
j. Southeastern USA Plains
k. Mississippi Alluvial And Southeast USA Coastal Plains
l. Ozark/Ouachita-Appalachian Forested Mountains
m. Mixed Wood Plains
n. Atlantic Highlands
Days/°C
3
0
−3
MAR
JUN
SEP
Mean Flowering Date
Apparent adaptation (S_{space} - S_{time})
Apparent plasticity (S_{time})

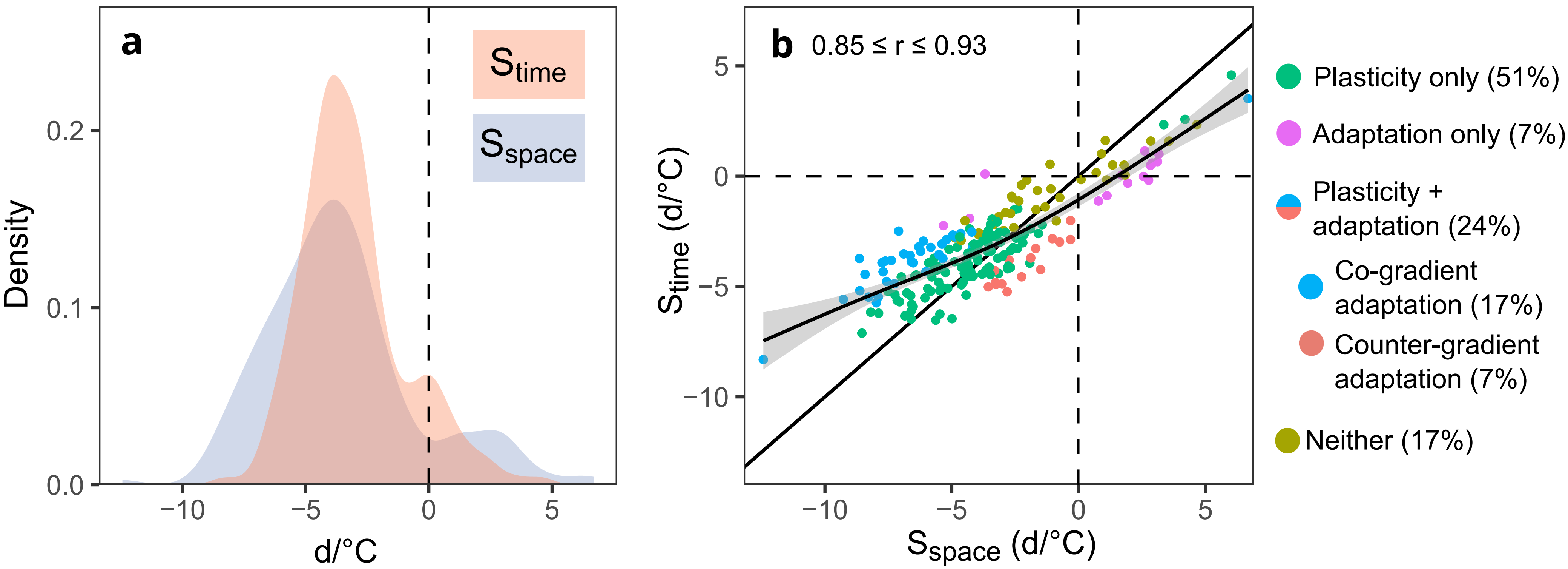

a
S_{time}
S_{space}
Density
0.0
0.1
0.2
−10
−5
0
5
d/°C
b
0.85 ≤ r ≤ 0.93
S_{time} (d/°C)
5
0
−5
−10
−10
−5
0
5
S_{space} (d/°C)
Plasticity only (51%)
Adaptation only (7%)
Plasticity + adaptation (24%)
Co-gradient adaptation (17%)
Counter-gradient adaptation (7%)
Neither (17%)

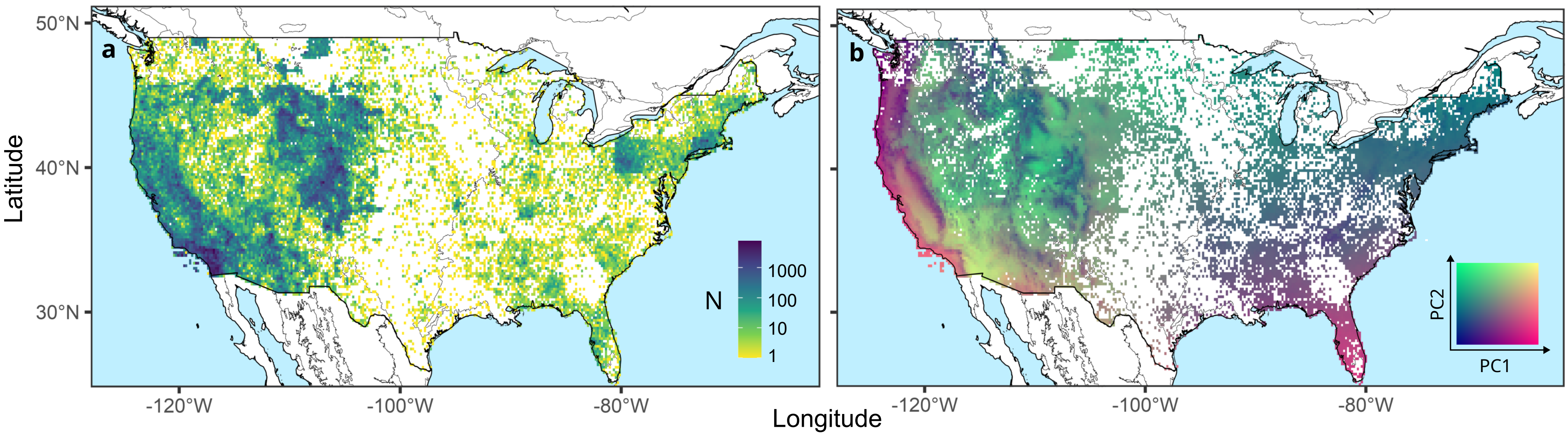
a
b
50°N
40°N
30°N
Latitude
-120°W
-100°W
-80°W
Longitude
N
1000
100
10
1
PC2
PC1

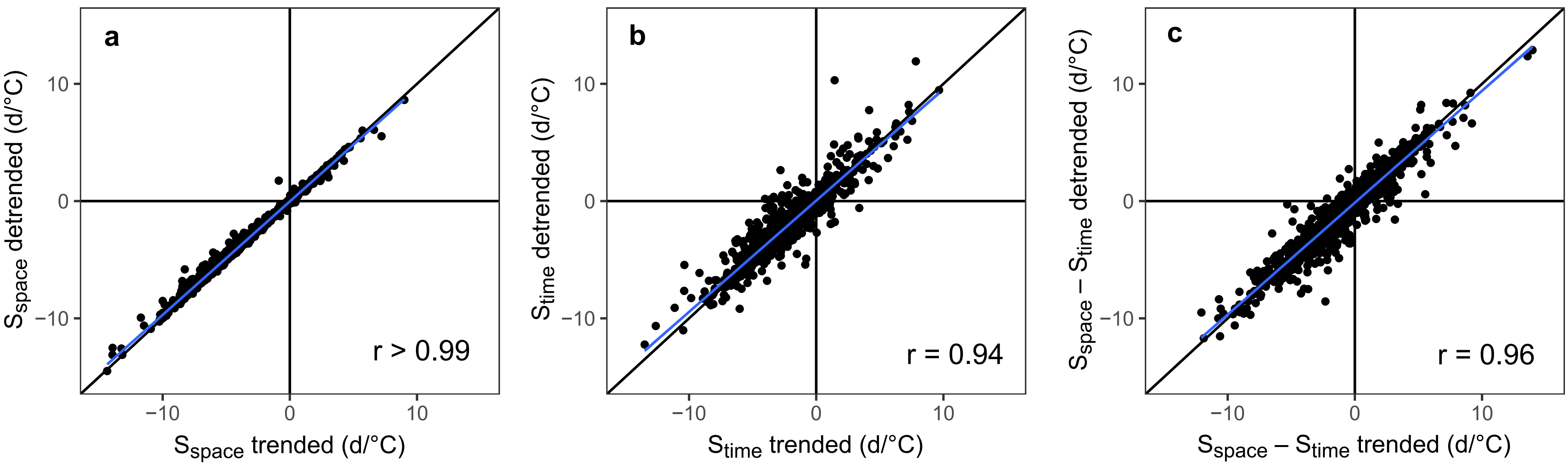

a
r > 0.99
S_{space} detrended (d/°C)
S_{space} trended (d/°C)
b
r = 0.94
S_{time} detrended (d/°C)
S_{time} trended (d/°C)
c
r = 0.96
$S_{space} - S_{time}$ detrended (d/°C)
$S_{space} - S_{time}$ trended (d/°C)

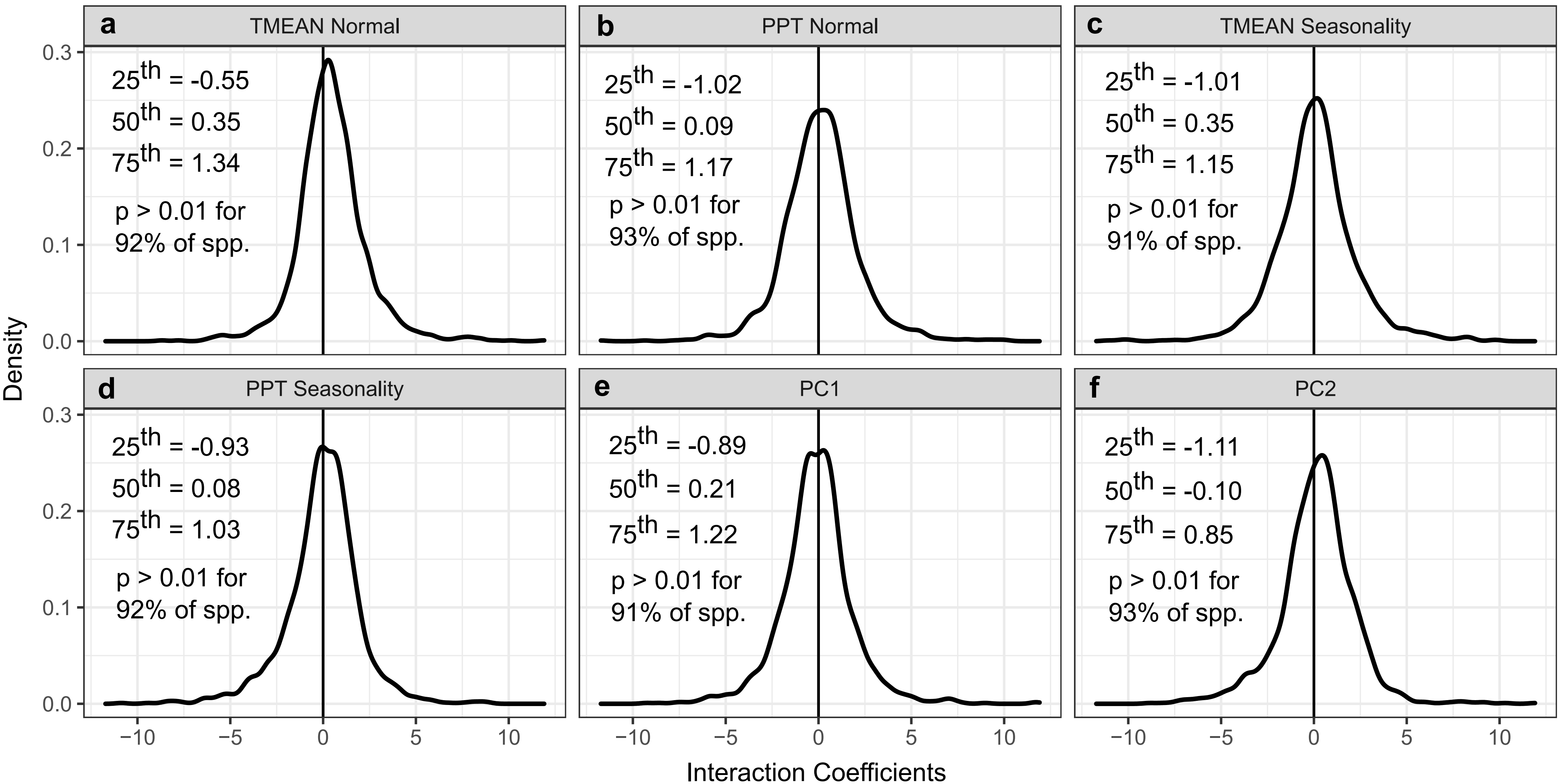

a
TMEAN Normal
25th = -0.55
50th = 0.35
75th = 1.34
p > 0.01 for
92% of spp.
b
PPT Normal
25th = -1.02
50th = 0.09
75th = 1.17
p > 0.01 for
93% of spp.
c
TMEAN Seasonality
25th = -1.01
50th = 0.35
75th = 1.15
p > 0.01 for
91% of spp.
d
PPT Seasonality
25th = -0.93
50th = 0.08
75th = 1.03
p > 0.01 for
92% of spp.
e
PC1
25th = -0.89
50th = 0.21
75th = 1.22
p > 0.01 for
91% of spp.
f
PC2
25th = -1.11
50th = -0.10
75th = 0.85
p > 0.01 for
93% of spp.
Density
Interaction Coefficients
0.0
0.1
0.2
0.3
−10
−5
0
5
10

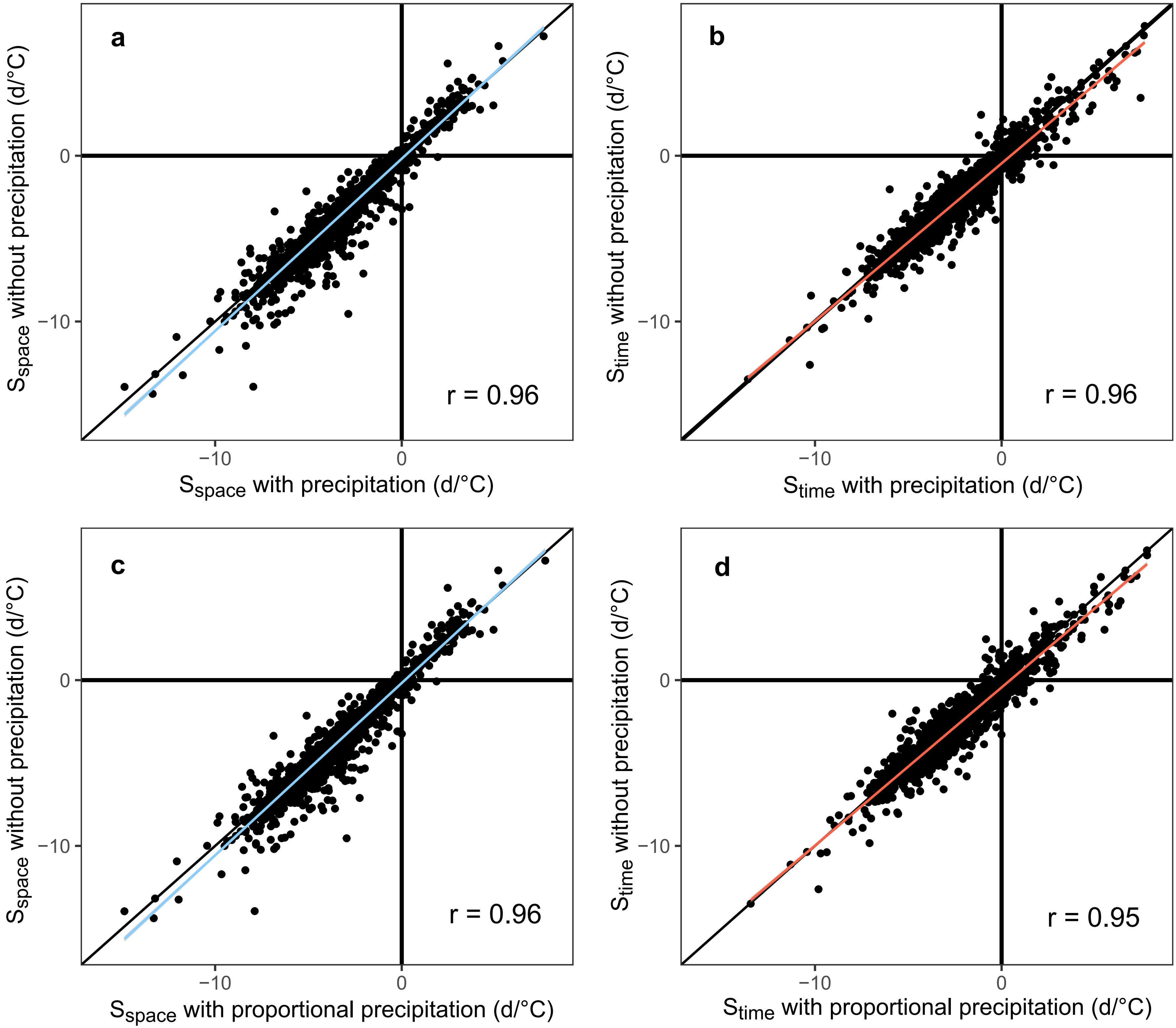
a
b
c
d
r = 0.96
r = 0.96
r = 0.96
r = 0.95
0
−10
S_{space} without precipitation (d/°C)
S_{space} with precipitation (d/°C)
S_{time} without precipitation (d/°C)
S_{time} with precipitation (d/°C)
S_{space} with proportional precipitation (d/°C)
S_{time} with proportional precipitation (d/°C)

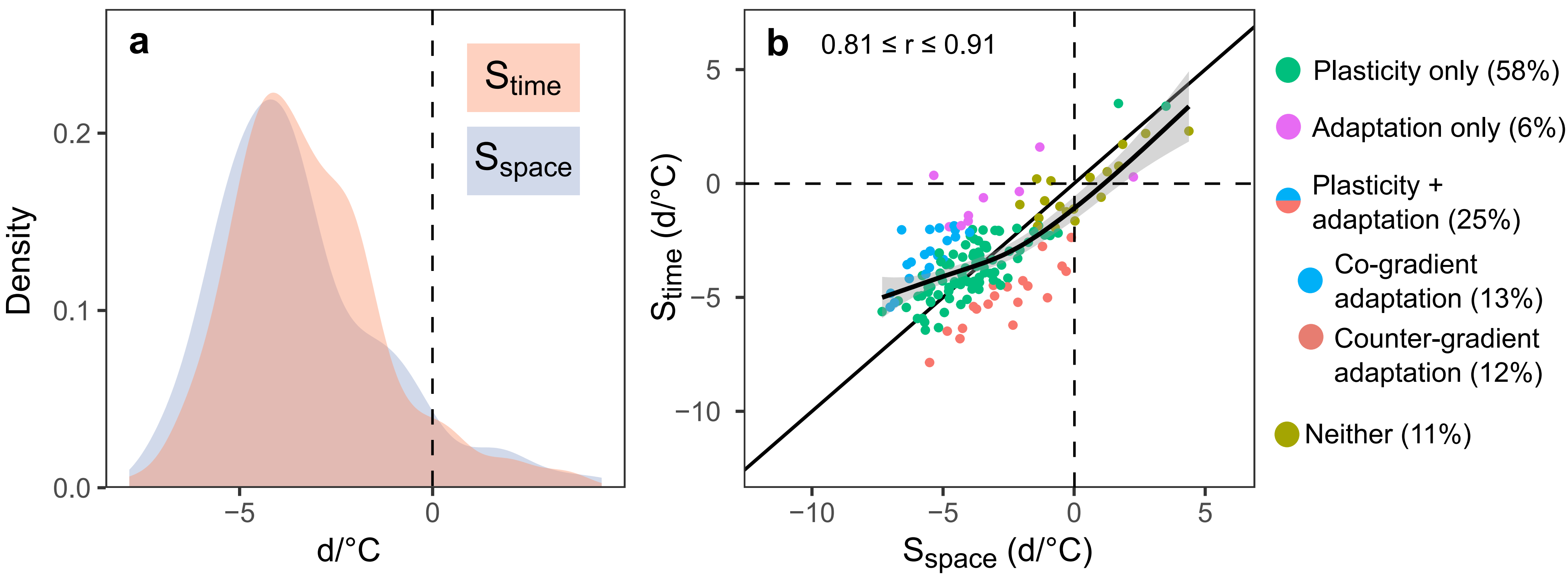

a
Density
0.0
0.1
0.2
−5
0
d/°C
S_time
S_space
b
0.81 ≤ r ≤ 0.91
S_time (d/°C)
5
0
−5
−10
−10
−5
0
5
S_space (d/°C)
Plasticity only (58%)
Adaptation only (6%)
Plasticity + adaptation (25%)
Co-gradient adaptation (13%)
Counter-gradient adaptation (12%)
Neither (11%)

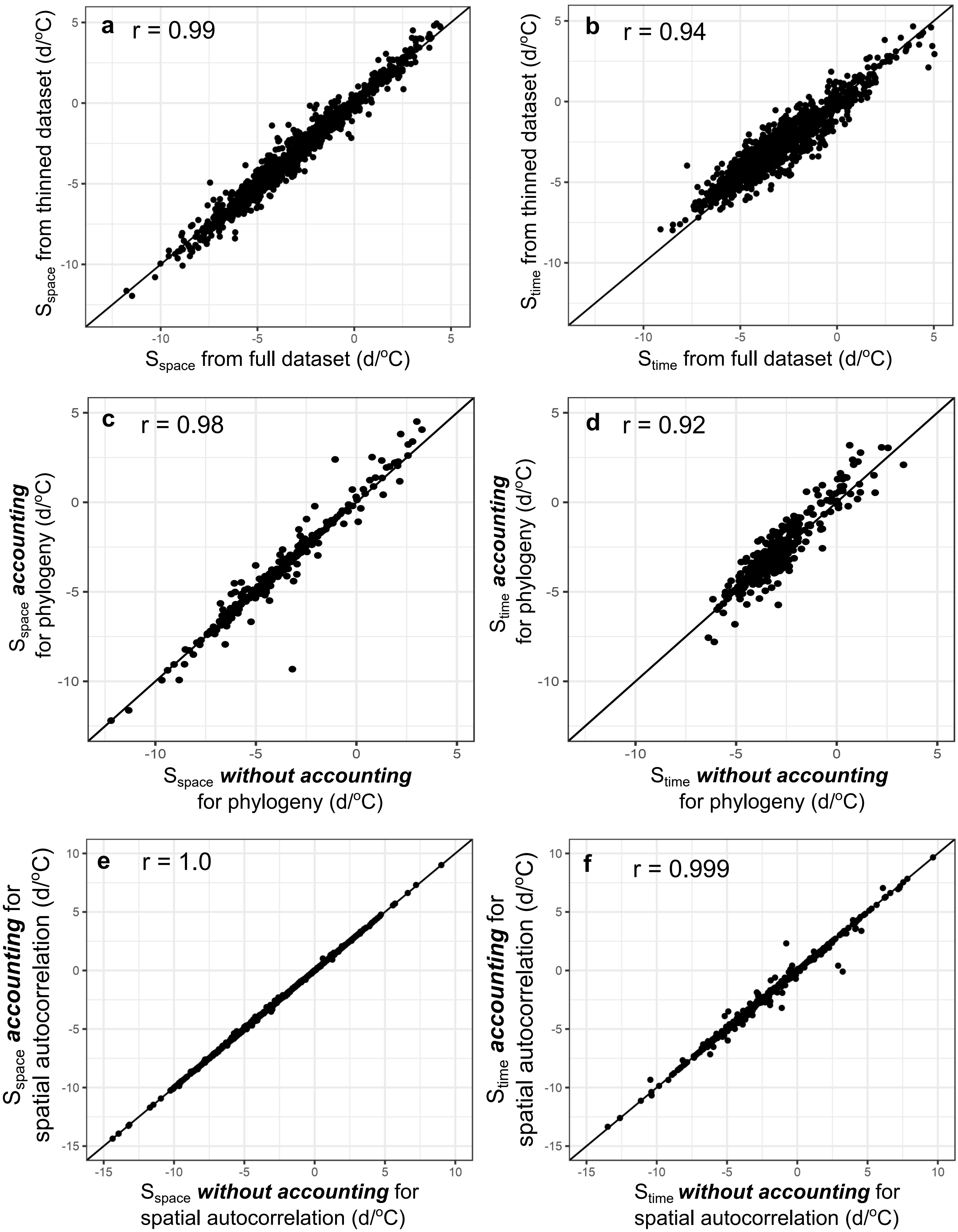
a
r = 0.99
S_{space} from thinned dataset (d/°C)
S_{space} from full dataset (d/°C)
b
r = 0.94
S_{time} from thinned dataset (d/°C)
S_{time} from full dataset (d/°C)
c
r = 0.98
S_{space} ***accounting*** for phylogeny (d/°C)
S_{space} ***without accounting*** for phylogeny (d/°C)
d
r = 0.92
S_{time} ***accounting*** for phylogeny (d/°C)
S_{time} ***without accounting*** for phylogeny (d/°C)
e
r = 1.0
S_{space} ***accounting*** for spatial autocorrelation (d/°C)
S_{space} ***without accounting*** for spatial autocorrelation (d/°C)
f
r = 0.999
S_{time} ***accounting*** for spatial autocorrelation (d/°C)
S_{time} ***without accounting*** for spatial autocorrelation (d/°C)

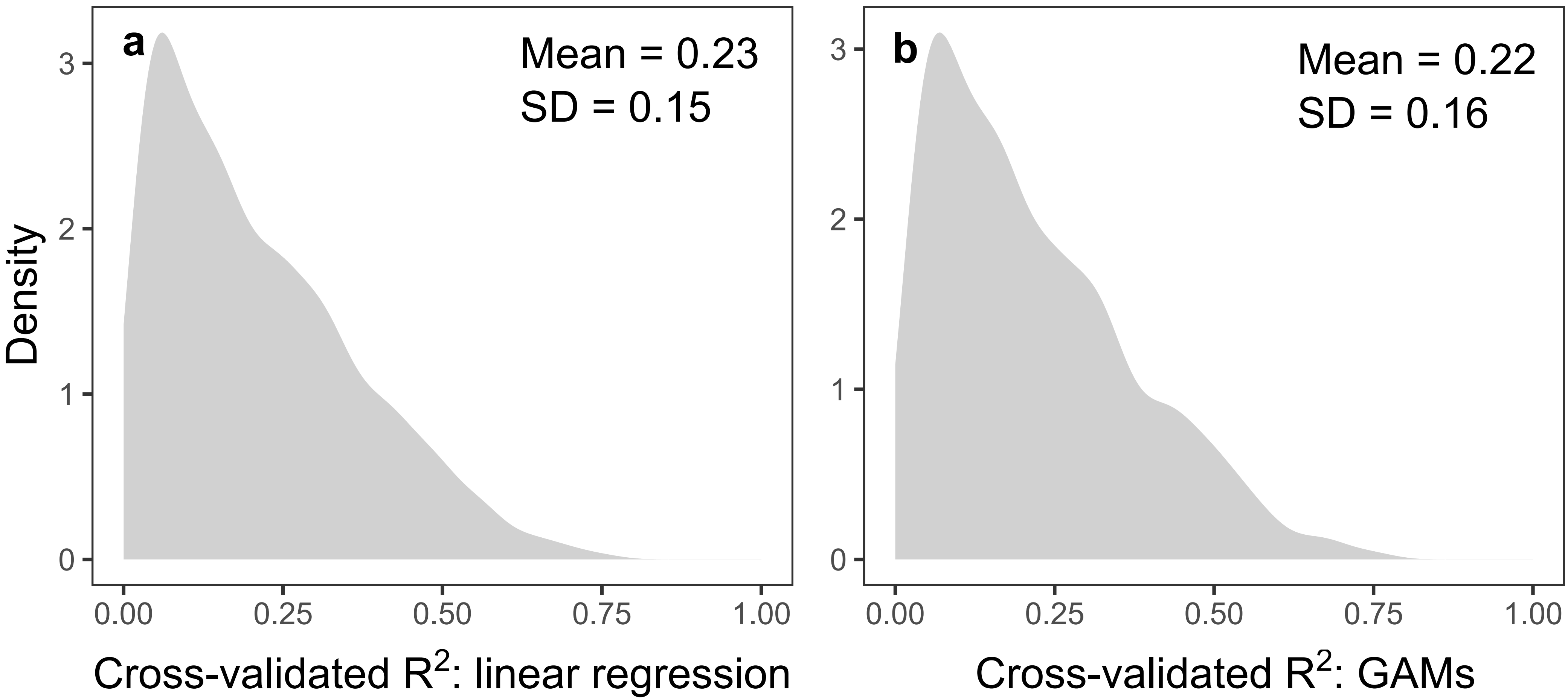
a
Mean = 0.23
SD = 0.15
Density
0
1
2
3
0.00
0.25
0.50
0.75
1.00
Cross-validated R^2: linear regression
b
Mean = 0.22
SD = 0.16
0
1
2
3
0.00
0.25
0.50
0.75
1.00
Cross-validated R^2: GAMs

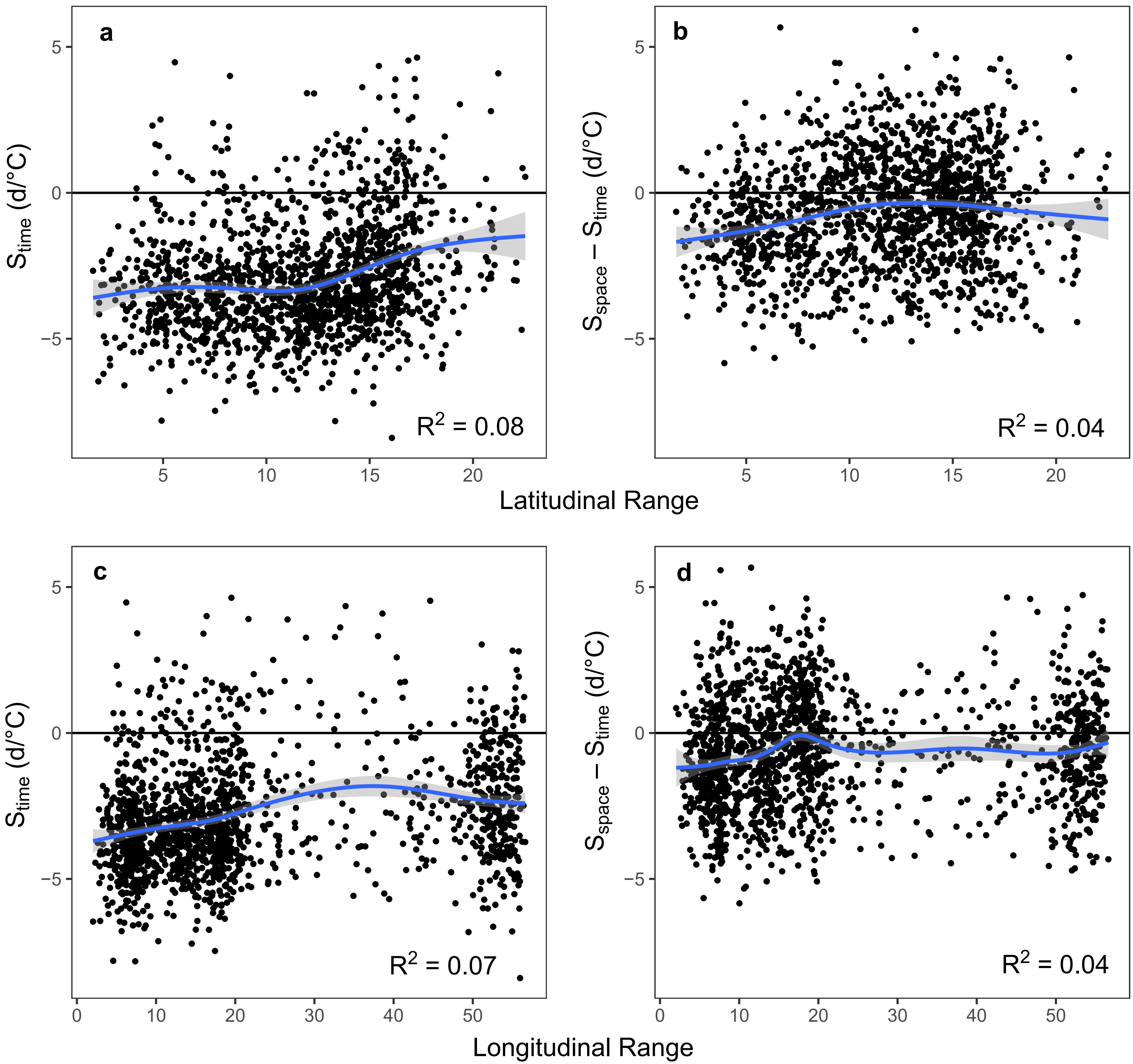
a
b
c
d
S_{time} (d/°C)
$S_{space} - S_{time}$ (d/°C)
$R^2 = 0.08$
$R^2 = 0.04$
$R^2 = 0.07$
$R^2 = 0.04$
Latitudinal Range
Longitudinal Range
5
0
−5
10
15
20
30
40
50

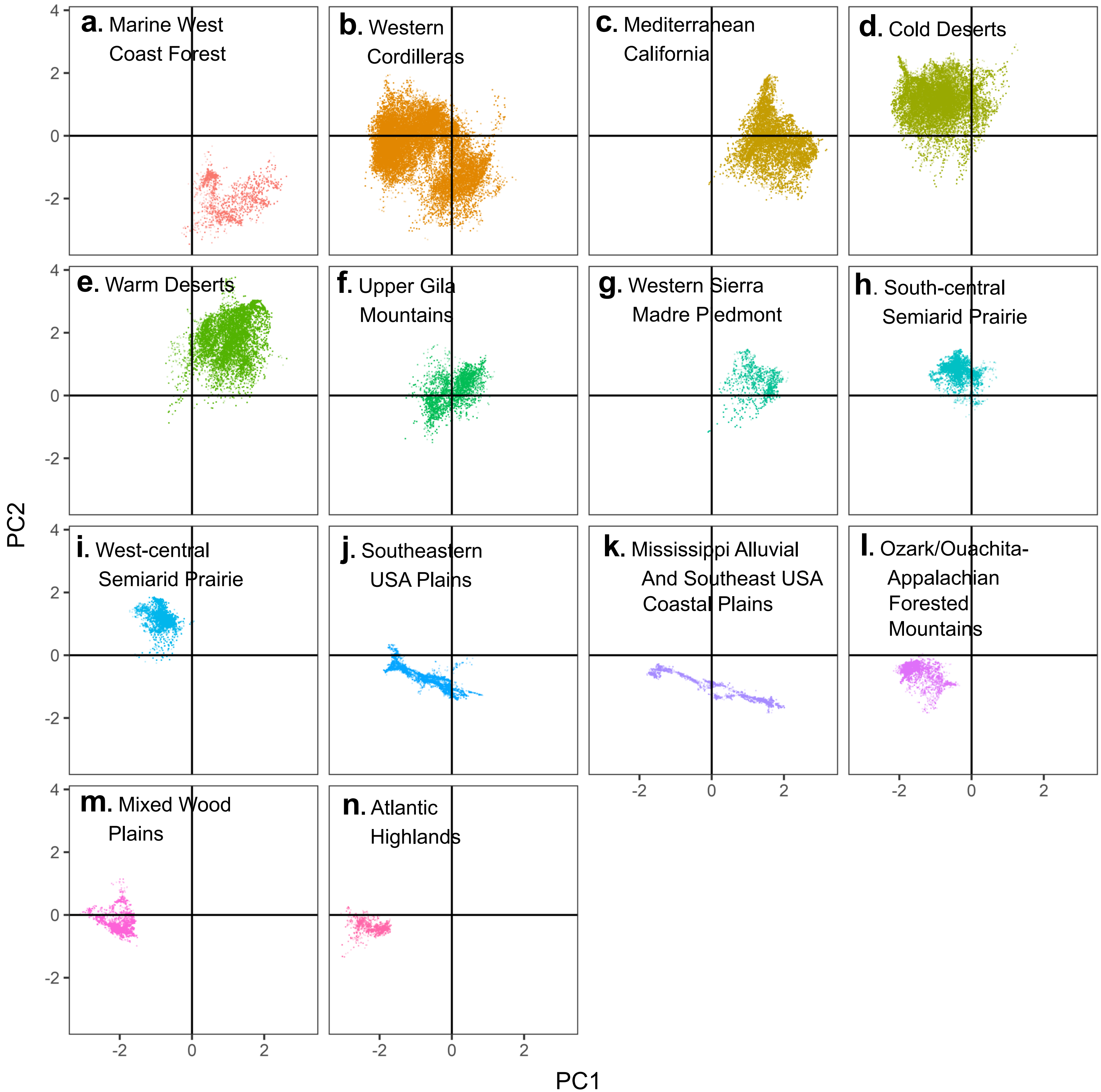
a. Marine West Coast Forest
b. Western Cordilleras
c. Mediterranean California
d. Cold Deserts
e. Warm Deserts
f. Upper Gila Mountains
g. Western Sierra Madre Piedmont
h. South-central Semiarid Prairie
i. West-central Semiarid Prairie
j. Southeastern USA Plains
k. Mississippi Alluvial And Southeast USA Coastal Plains
l. Ozark/Ouachita-Appalachian Forested Mountains
m. Mixed Wood Plains
n. Atlantic Highlands
PC1
PC2
4
2
0
-2